Development of a Total Internal Reflection Illumination System for Fluorescence Correlation Spectroscopy

Alexandria Doerfler
Advisor: Dr. James L. Thomas

Undergraduate Honors Research Thesis
University of New Mexico Physics and Astronomy
May 8, 2015

Abstract

Many cell surface receptors consist of multiple subunits that non-covalently associate to form a complete receptor. The integrin receptor is one such example. It is hypothesized that a drug (Thioridazine) that inhibits the binding of this receptor to its ligand functions by causing the dissociation of the two subunits. We have explored the use of fluorescence microscopy in several modalities to test this hypothesis. Firstly, direct imaging of fluorescently labeled receptor subunits was attempted, using image correlation analysis and distinct fluorescent tags for each subunit. Low signal levels prevented this approach from working, so we redesigned the experiment to use a single, diffraction-limited laser-illuminated spot on the cell membrane. With micron-sized spot illumination, the association of the two-receptor subunits would be revealed by correlated temporal fluctuations in the fluorescence signals in both channels. Unfortunately, intrinsic, internal cellular fluorescence dominated the signal. To reduce this intrinsic background, we used two approaches to use an evanescent wave from total internal reflection (TIR) for illumination: through-objective TIR and external TIR. The latter was successful, as demonstrated by measuring the fluorescence excited in a dye solution as the incident angle was varied.

Table of Contents

Introduction

The VLA-4 protein (also known as the integrin receptor) is a cell membrane protein made up of two subunits, α_4 and β_1, and its main function is to regulate the movement of immune cells through the extracellular matrix to sites of inflammation.[1] The extracellular matrix consists of fibrous proteins and polysaccharides and provides structural support to tissues; VLA-4 naturally binds to two different extracellular matrix ligands, VCAM-1 and Fibronectin. This binding is known to occur between the protein and its ligands during chronic inflammatory diseases (e.g. rheumatoid arthritis, transplant reject, allergies, etc…).[1,2] Blocking the interaction between VLA-4 and its ligands is a target for potential drug therapies to treat inflammatory diseases, prevent growth of new blood vessels (as occurs with a cancer tumor), and prevent the growth of blood clots.[1,2] It is known that the drug Thioridazine (common name Mellaril) blocks the binding of VLA-4 to its ligands.[1] However, the mechanism behind this blockade is unknown. It is hypothesized that Thioridazine blocks the binding between the sub-units, α_4 and β_1, thus preventing the binding of VLA-4 to its ligands (Figure 1).

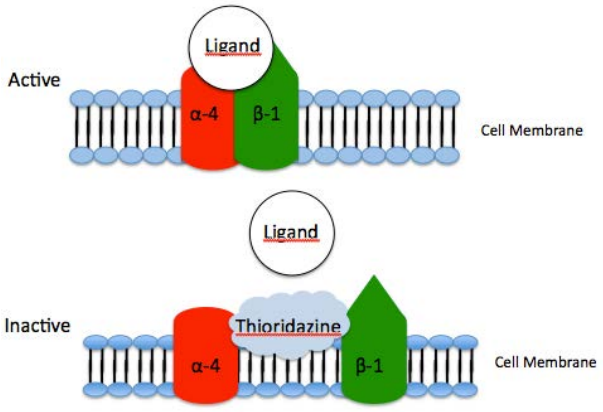

Figure 1.
The dissociation between α_4 and β_1 is a target for existing drug therapies as the binding between the VLA-4 protein and its ligands is known to occur during chronic inflammatory diseases. The drug Thioridazine is hypothesized to prevent the interaction between VLA-4 and its ligands through the dissociation of its subunits, α_4 and β_1.

To study whether receptor subunits are associated, it is necessary to have specific labels that allow them to be detected in a microscope. The most commonly used method to specifically label a particular protein or subunit is to use an antibody molecule that recognizes and binds to a specific site on the subunit of interest. Antibodies are natural immune proteins that bind to foreign molecules

through van der Waals and electrostatic forces. Only certain antibodies will attach themselves to specific foreign molecules, and thus only one type of antibody will attach itself to α_4 and a different type of antibody will attach itself to β_1. Each antibody must be attached to a reporter that will generate a unique signal in microscopy: for example, an organic fluorescent dye, a quantum dot, or a gold nanoparticle. In this project, three dye molecules were used: Alexa488 (excitation at 495 nm, emission at 519 nm), Cy 5 (excitation at 650 nm, emission at 670 nm), and phycoerythrin (PE) (excitation at 565 nm, emission at 573).[6] Our collaborators (Drs. Chigaev and Smagley of the UNM Department of Pathology) covalently attached these dyes to the antibody molecules in a test tube reaction and purified the labeled antibodies. The labeled antibodies were then allowed to bind to cells to label the α_4 or β_1 subunits.

This project explored several techniques, all using fluorescence microscopy, to ascertain the extent of association between the α_4 and β_1 subunits, and to enable a determination of whether Thioridazine affects that association. The most "intuitive", straightforward method is simply to image the distribution of the receptor subunits on the cell membrane, and to determine the extent to which both subunits share the same distribution. This method will be discussed first; ultimately, it was not successful, so an alternative method using laser illumination was studied, which uses temporal, rather than spatial, correlation analysis. Issues with cellular background fluorescence required further modification to an evanescent wave illumination system. This can, in principle, be done through the objective or externally. The external illumination system proved to be successful, as demonstrated by change in fluorescence from a test solution on changing incident angle.

Experiments

Image Correlation Spectroscopy

The first method used for this project was Image Correlation Spectroscopy (ICS). It is based on the idea that similarity in the spatial distributions of the two subunits reflects the extent to which the subunits are associated. Even if the receptors are randomly distributed in the fluid cell membrane, there will be Poisson fluctuations in their concentrations, and these fluctuations will be correlated if the subunits are associated.

In Image Correlation Spectroscopy, both spatial and temporal correlations between images can be calculated. The correlation is calculated using the intensity data held in the image pixels. The general spatiotemporal intensity fluctuation correlation function is

$$r_{ab}(\xi,\eta,\tau) = \frac{\langle \delta i_a(x,y,t)\delta i_b(x+\xi,y+\eta,t+\tau)\rangle}{\langle i_a\rangle_t \langle i_b\rangle_{t+\tau}} \quad (1)$$

where ξ,η are spatial lag variables and τ is a temporal lag variable, and the subscripts a and b correspond to two different channels.[11,12,13] Spatial and temporal cross-correlation are treated separately in ICS. The spatial correlation is defined as the general spatiotemporal function at zero time lag,

$$r_{ab}(\xi,\eta,0) = \frac{\langle \delta i_a(x,y,t)\delta i_b(x+\xi,y+\eta,t)\rangle}{\langle i_a\rangle_t \langle i_b\rangle_{t+\tau}} \quad (2)$$

and the temporal correlation is defined as the general spatiotemporal function at zero spatial lag[11,12,13] ,

$$r_{ab}(0,0,\tau) = \frac{\langle \delta i_a(x,y,t)\delta i_b(x,y,t+\tau)\rangle}{\langle i_a\rangle_t \langle i_b\rangle_{t+\tau}} \quad (3)$$

For randomly distributed receptors, there is no spatial correlation in receptor locations, and one might expect the spatial correlation function to be a delta function at zero spatial lag. (The delta function arises from each receptor's correlation with itself). However, because the microscope has a finite resolution, the spatial correlation function has a finite width. This resolution width is usually modeled as a Gaussian, rather than the more complicated autocorrelation of an Airy function. With a random receptor distribution and a Gaussian model, the two-dimensional spatial correlation function is:

$$r_{ab}(\xi,\eta,0) = g_{ab}(0,0,0)e^{\left(-\frac{\xi^2+\eta^2}{\omega_{2pab}^2}\right)} + g_{\infty ab} \qquad (4)$$

where $e^{\left(-\frac{\xi^2+\eta^2}{\omega_{2pab}^2}\right)}$ represents the effect of the diffraction limit of the microscope, and subscripts a and b represent channels (a=b for autocorrelation), $g_{ab}(0,0,0)$ is the zero-lag amplitude, and $g_{\infty abn}$ is the offset.[11,12,13] For cross-correlation, the width of the Gaussian depends on the resolution for each channel, but for nearby emission wavelengths this may be assumed to be the same.

For practice in analyzing image data, a four-dimensional array of model images was created with the form (x, y, color, time). In this array, color has the values of 1 or 2, time has values of 1 to 60 units, and x and y go between 1 and 104 pixels. There are 200 proteins of each color, and a significant number of them are bound together. The proteins are located on a 100x100 lattice and diffuse over time. At each time point, each subunit distribution was convolved with a Gaussian point spread function to simulate diffraction in the microscope. (That also increased the image size to 104x104.) There is also a modest background (20% of the single fluorophore counts) and Poisson noise was added to every pixel. The spatiotemporal correlation analysis for ICS as described above was used to analyze this model of images (Matlab program is in Appendix 2.1). First, the model images were auto-correlated at five and ten frame lags, and then fit according to equation (3) above. The results of the autocorrelations and fits are shown in Figures 1a, 1b,

2a, and 2b. The figures are three-dimensional Matlab plots, and each color corresponds to a different cross section in the three dimensional correlation.

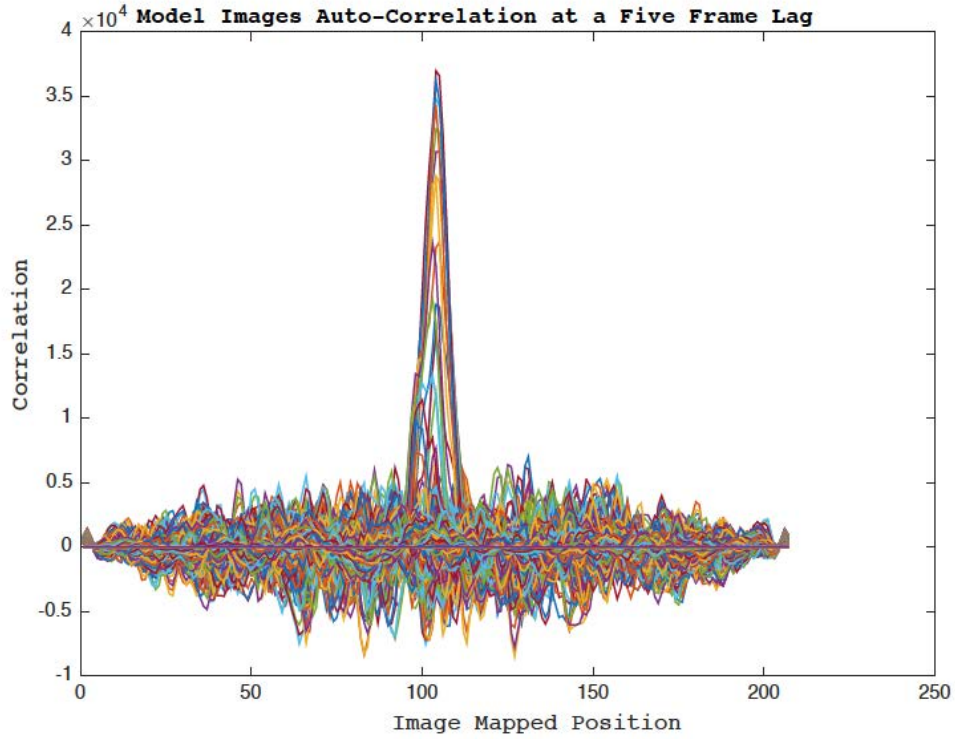

Figure 1a.
The result of auto-correlating the model images at a five frame lag. The plot is a three dimensional Matlab plot, and each color displays a different cross section in the correlation. The width of the Gaussian is a result of both the diffraction limit and the spreading of fluorophores by diffusion.

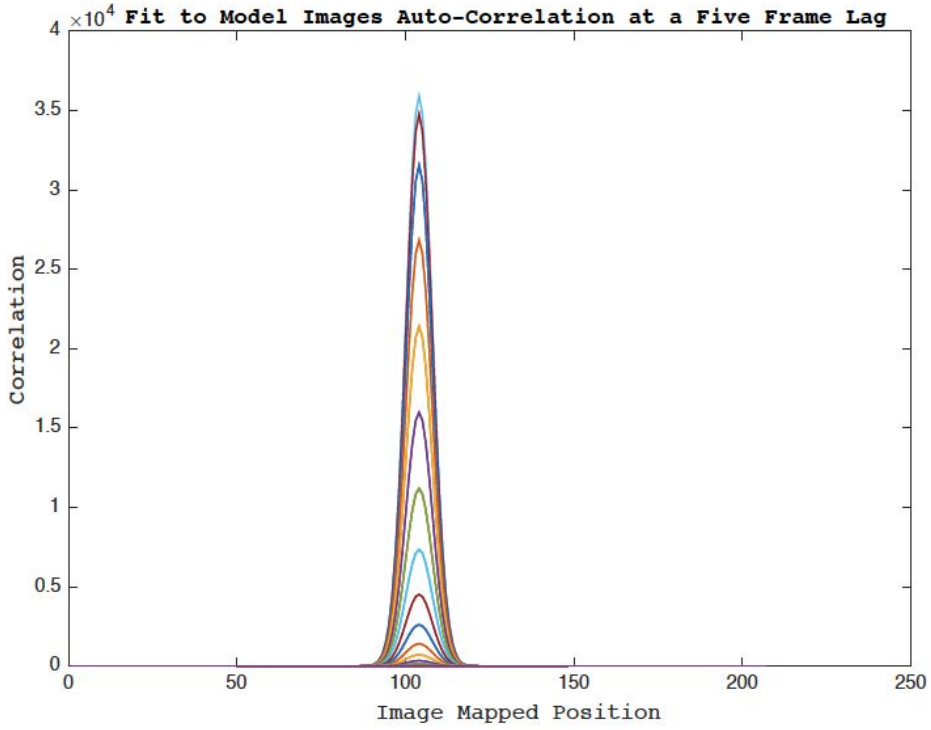

Figure 1b.
This plot displays the result of fitting Figure 1a to (3) above. Again, the fit is a three dimensional Matlab plot, and each color displays a different cross section in the correlation.

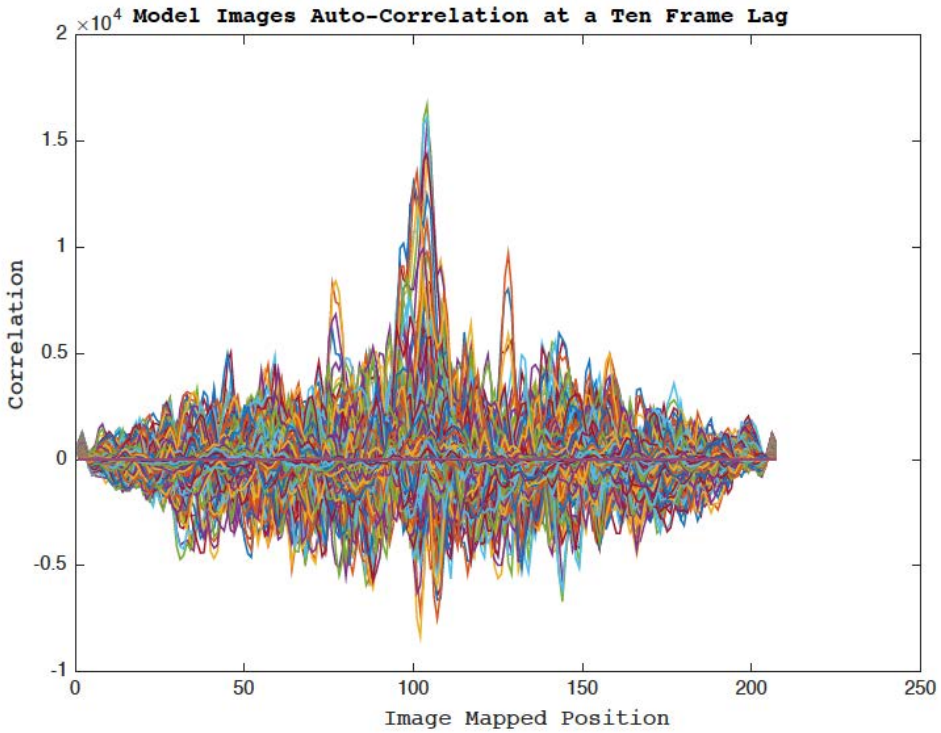

Figure 2a.
The result of auto-correlating the model images at a ten-frame lag. Note that the amplitude is approximately half as it was at a five frame lag, and the width has increased, which is expected for diffusion. The plot is a three dimensional Matlab plot, and each color displays a different cross section in the correlation.

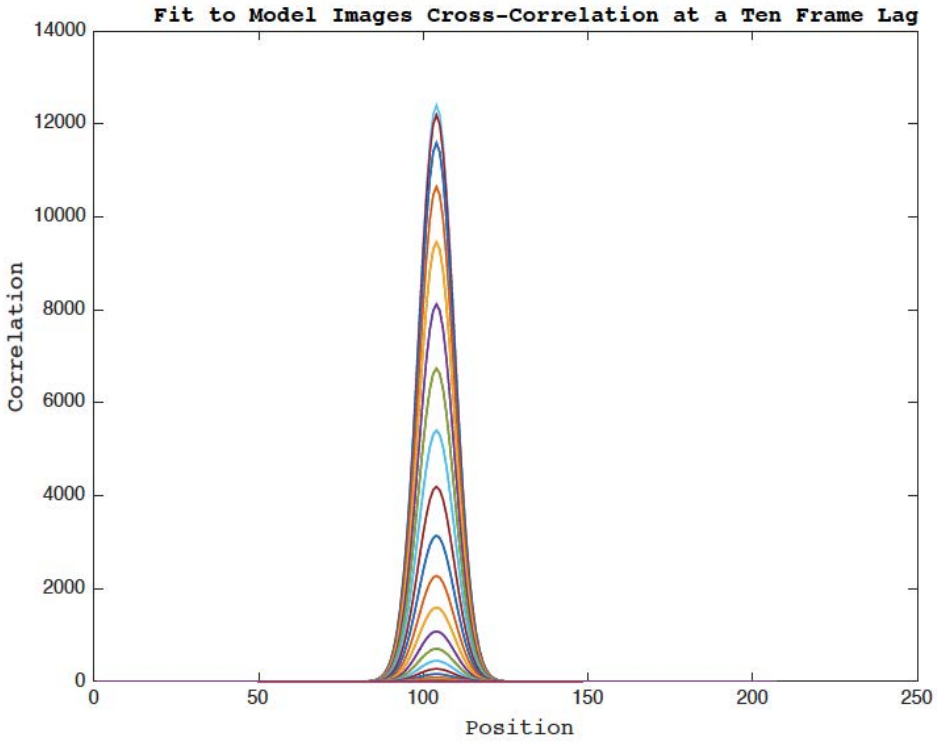

Figure 2b.
The result of fitting to the auto-correlation of at a ten frame lag. The fit is a three dimensional Matlab plot, and each color displays a different cross section in the correlation. Note that width has increased, compared to the 5 frame lag, by a factor of $\sqrt{2}$.

The model images were then cross-correlated at a zero-frame lag and fit to equation (4) above, as shown in Figures 3a-b.

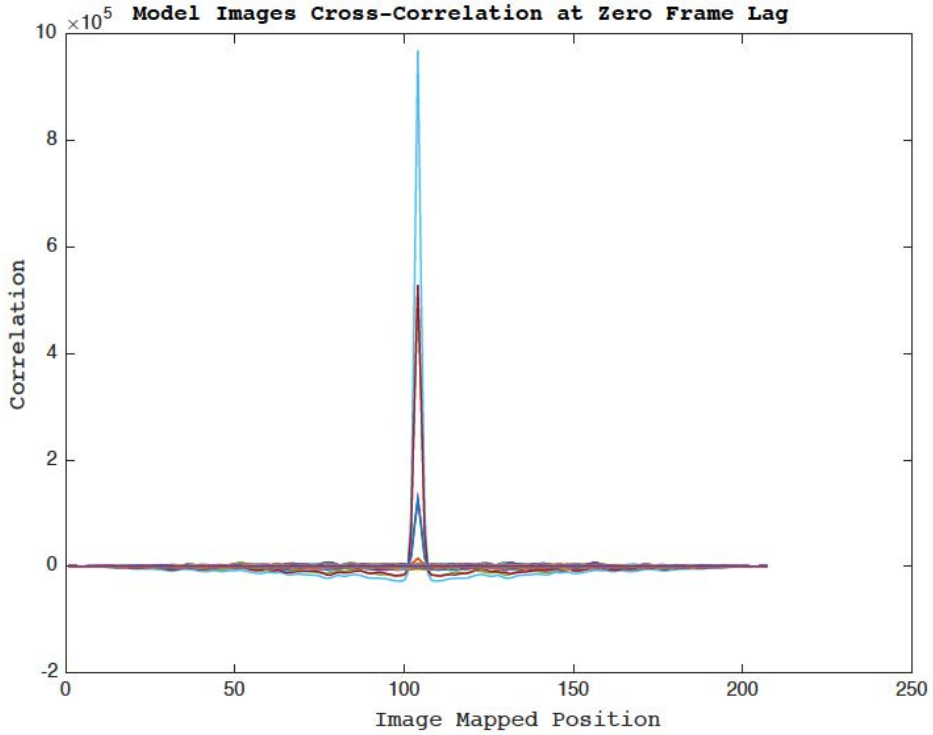

Figure 3a-1.
The result of cross correlating the model images at a zero-frame lag. The plot is a three dimensional Matlab plot, and each color displays a different cross section. The width of the Gaussian is a result of the diffraction in the microscope. Different colors represent different fractions of dimerized receptors.

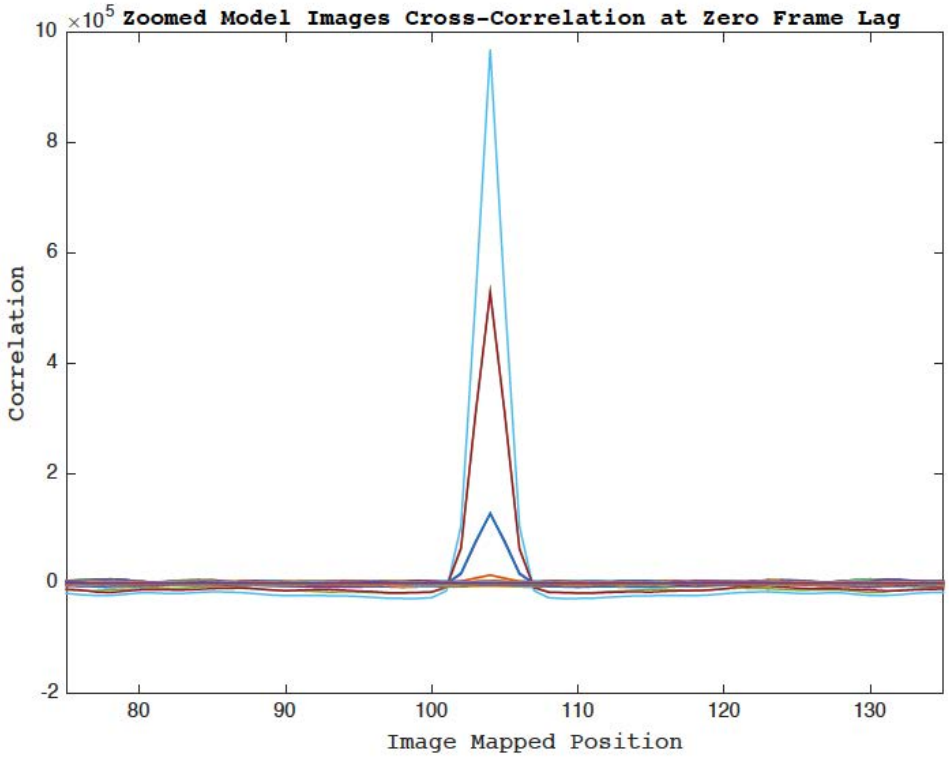

Figure 3a-2.
A zoomed image of the cross-correlation at zero frame lag.

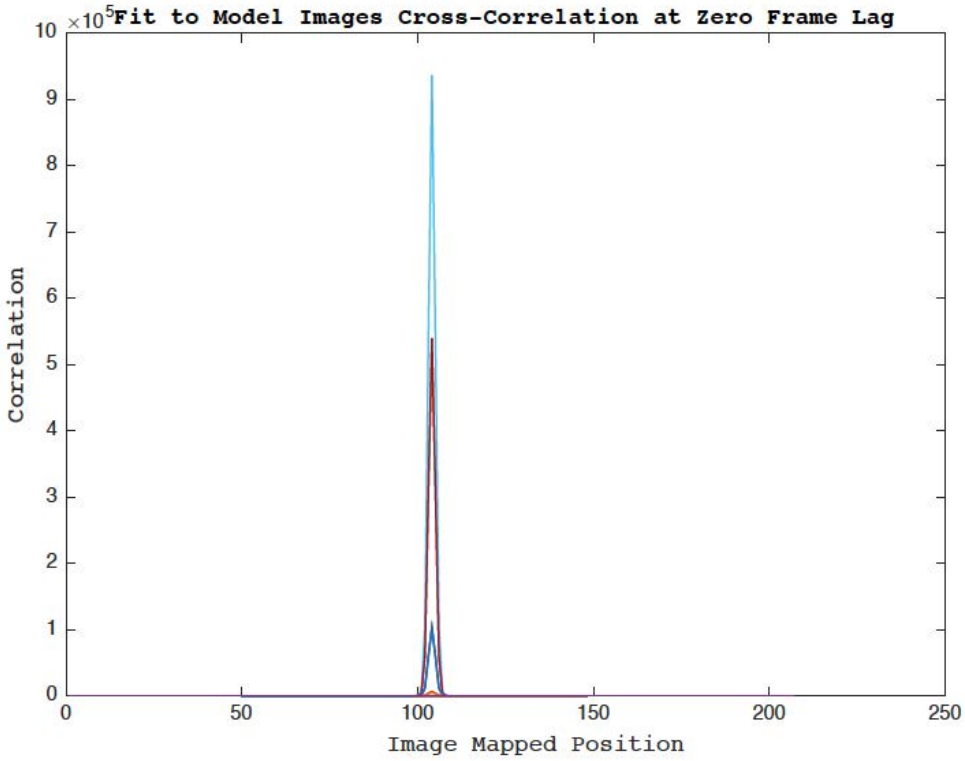

Figure 3b.
The result of fitting to the cross-correlation at a zero frame lag using equation (4) as described above.

The above autocorrelations, along with the fits, show that the width of each Gaussian curve becomes larger as the time lag increases. Figure 4 displays the linear progression of the squared width at 0, 5, and 10-frame time lags.

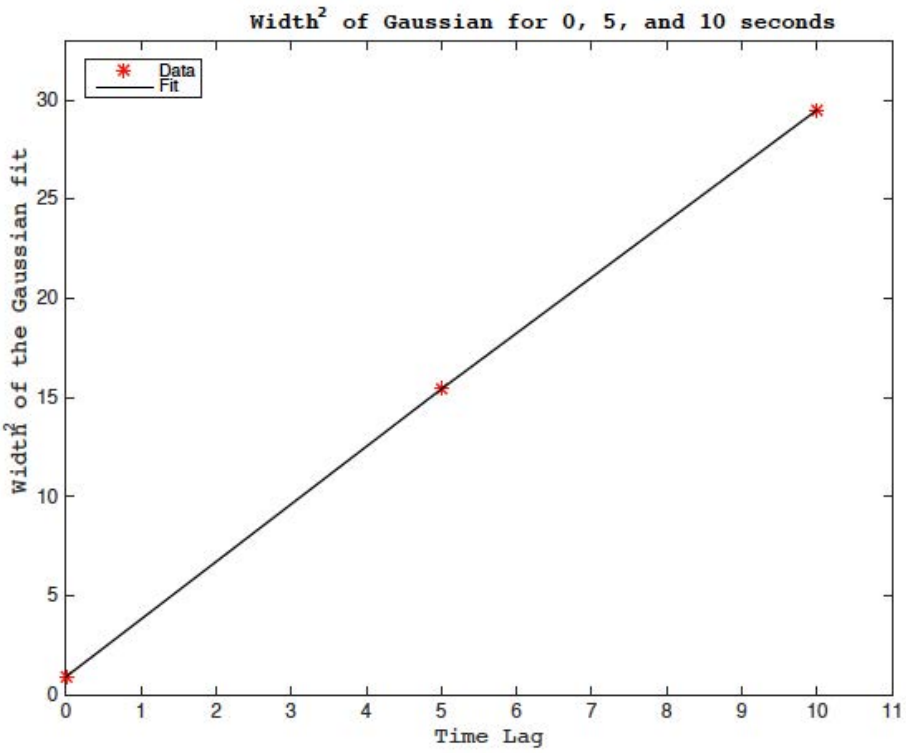

Figure 4.
The square of the width for each Gaussian curve at time lags 0, 5, and 10 frames depends linearly on time, as expected for a diffusive process.

The next step for the project was to analyze data taken from live cells. I worked in collaboration with Samantha Schwartz, a graduate student with Professor Keith Lidke. Image 1 displays a sample image taken in Professor Keith Lidke's lab.

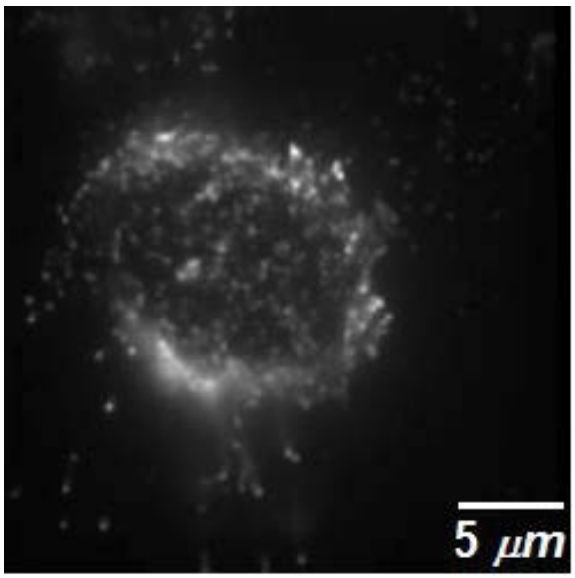

Image 1.
An example image taken during the ICS experiment of this project. This cell was labeled with Alexa488 anti-CLA4 Integrin antibody.

The fluorophores used in this part of the project were Alexa488 (label for alpha-4) and Cy5 (label for beta-1). While this was thought to be a promising technique for detecting the correlation between alpha-4 and beta-1, and Alexa488 gave a nice signal (as seen in Image1), problems arose with the signal from Cy5, as it was difficult to detect in the microscope. Furthermore, the effects of photobleaching (a process in which the fluorescence of a fluorophore is abolished in an excited state reaction) hindered our ability to accurately detect each fluorophore after only a few minutes.

To obtain higher signals from Cy5, we decided to use spot illumination with a laser source. Rather than monitor spatial distributions, the temporal fluctuations in signals can be correlated to determine the extent of receptor associations. The fluctuations arise from the lateral diffusion of proteins in the fluid cell membrane. Furthermore, if a photon count record could be taken of the fluorescence intensity, then it may be possible to correct for photobleaching. Fluorescence Correlation Spectroscopy (FCS) was thus the next step in trying to develop a system for detecting the association between alpha-4 and beta-1.

Fluorescence Correlation Spectroscopy

As stated, it was believed that FCS might be a better technique for determining the dissociation of alpha-4 and beta-1 as a laser spot directly on the cell could increase the fluorescence of Cy-5, and a photon history record could be used to correct for the effects of photobleaching. Photobleaching adversely affects the measurement of associations: both the fluorescent signal and the fraction of alpha-4 and beta-1 are not stationary during the course of the measurement, but decay over time. Thus, taking direct measurements of photon counts in both channels (instead of real time correlation), and making a dynamic estimate of dimer concentration using very short measurement intervals (properly accounting for the large uncertainties in measurement) followed by fitting to a model that includes photobleaching effects, will provide a way to correct for the loss of intensity during the data collection process. A Labview program was created (see Appendix 2.4) to

take a photon history record for each channel. The theory for this part of the project has not been completed yet.

In the lab of Dr. Thomas, an optical pathway was set up for the use of FCS, displayed in Figure 5 below (procedure as described in Appendix 1.1).

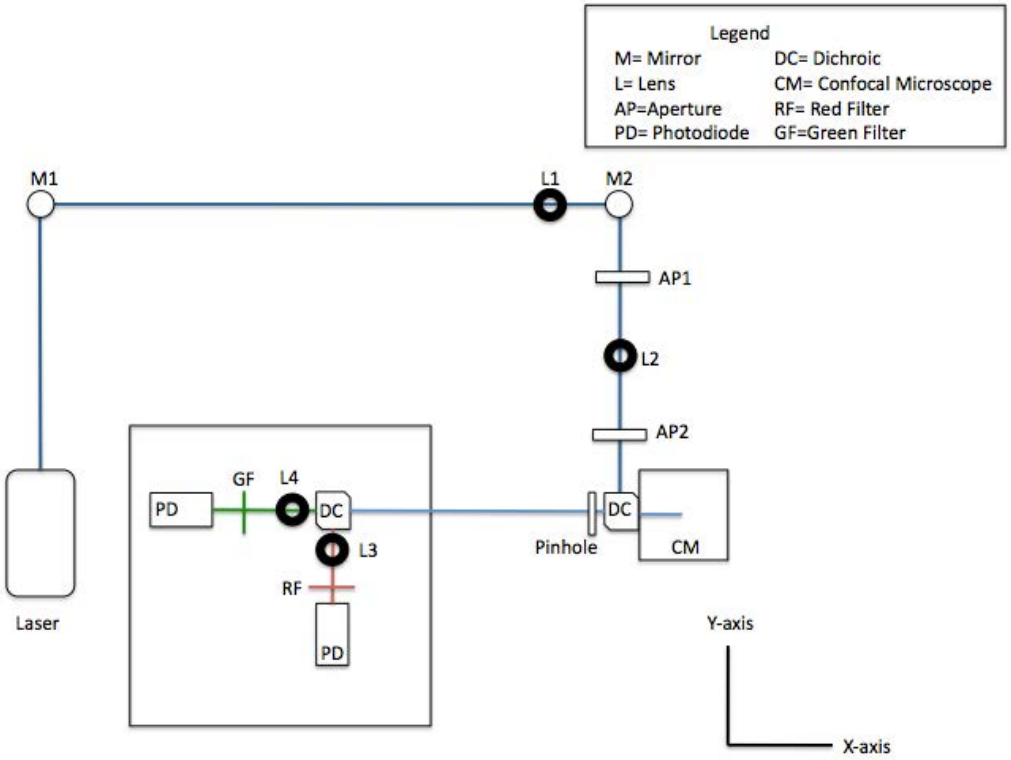

Figure 5.
Optical Set Up for FCS without TIR

Fluorescence correlation spectroscopy (FCS) measures fluorescence fluctuations, providing information about diffusion coefficients and concentrations of fluorophores.[1-5] The cell membrane is a two-dimensional fluid phospholipid bi-layer, and thus proteins in the cell membrane are (usually) free to diffuse laterally. The cross-correlation function for two-channel fluorescence correlation spectroscopy is

$$G_{ab}(\tau) = \frac{\langle \delta F_a(t) \delta F_b(t+\tau) \rangle}{\langle F_a(t) \rangle \langle F_b(t) \rangle} \qquad (5)$$

(a and b correspond to the two different channels, or two different labels).[1-5,8] If the two sub-units are bound together (correlated) then they will diffuse in and out of the detected field of view (FOV) together, and thus $\delta F_1(t)$ and $\delta F_2(t+\tau)$ will be both positive or both negative, thus always giving a positive result in the numerator.

However, if the two sub-units are unbound (uncorrelated) then $\delta F_1(t)$ and $\delta F_2(t+\tau)$ are as likely to have the same sign as they are to have an opposite sign, and thus the numerator will average to zero. By cross-correlating the intensity signal of the two different channels an estimate of the extent to which these specific receptor subunits are bound together in the cell membrane can be made.[1-5,8] In this part of the project, two differently colored labels (Alexa488 for alpha-4 and PE for beta-1) were used in an attempt to independently monitor the fluorescent fluctuations in alpha-4 and beta-1 using avalanche photodiodes for the fluorescence detection. See Figure 6 for a schematic of the measurement principle.

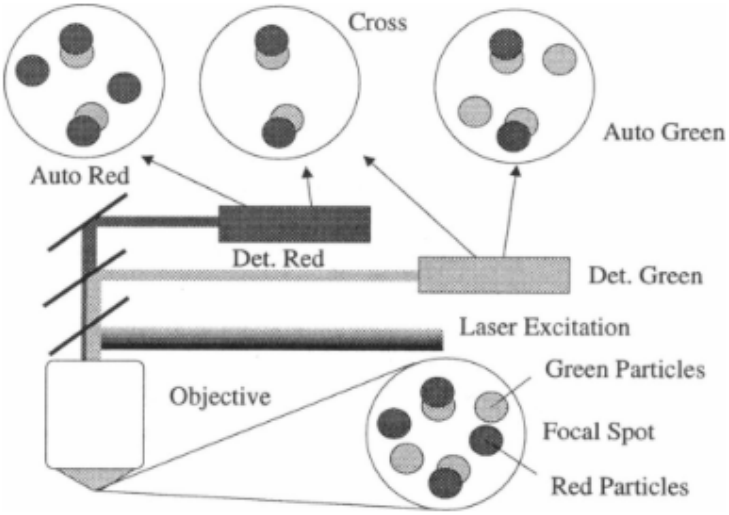

Figure 6.
Schematic of the measurement principle. A laser will illuminate the sample and the excitation from the two differently labeled fluorophores is transmitted onto two different detectors (red and green). In this case, the photodiode Det. Red detects red fluorescence and the photodiode Det. Green detects green fluorescence. The green fluorescence and red fluorescence data can then be auto correlated separately, while cross correlation will illuminate interactions between the labeled particles.
(from P. Schwille, F.J. Meyer-Almes, and R. Rigler, Biophysical Journal **72** (1997).)

Data was taken on live cells with no labeling, and cells in which alpha-4 was labeled with Alexa488. Figure 7a displays the measurements taken for the background photon count rate in a dark room, Figure 7b displays the photon count rate of cells that had no labeling, and Figure 7c displays the photon count rate of cells with the Alexa488 fluorescent labeling.

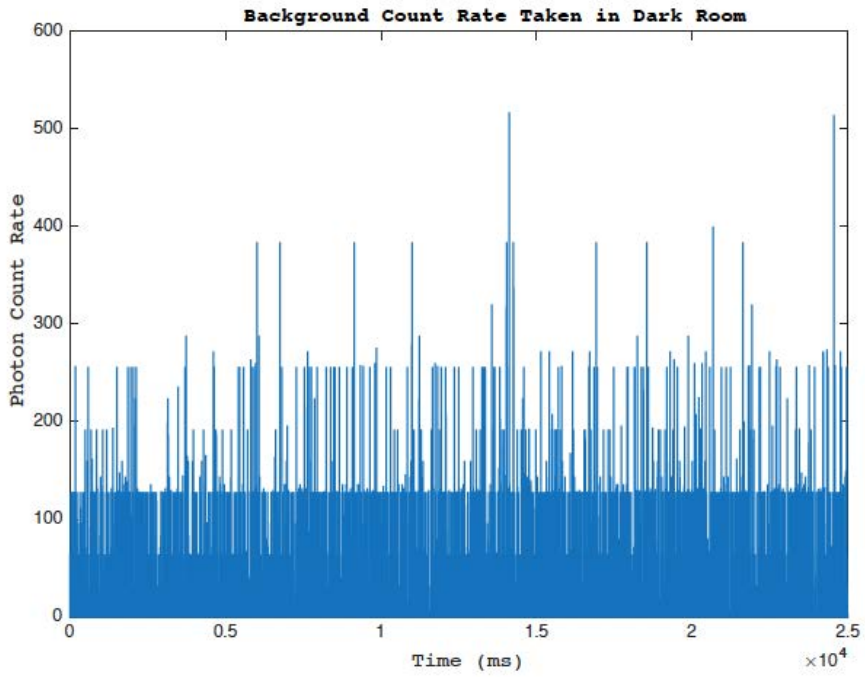

Figure 7a.
This graph displays the background (dark) count rate taken with one of the photodiodes in a dark room. The bin size is 16 ms, during which typically 2 counts occur.

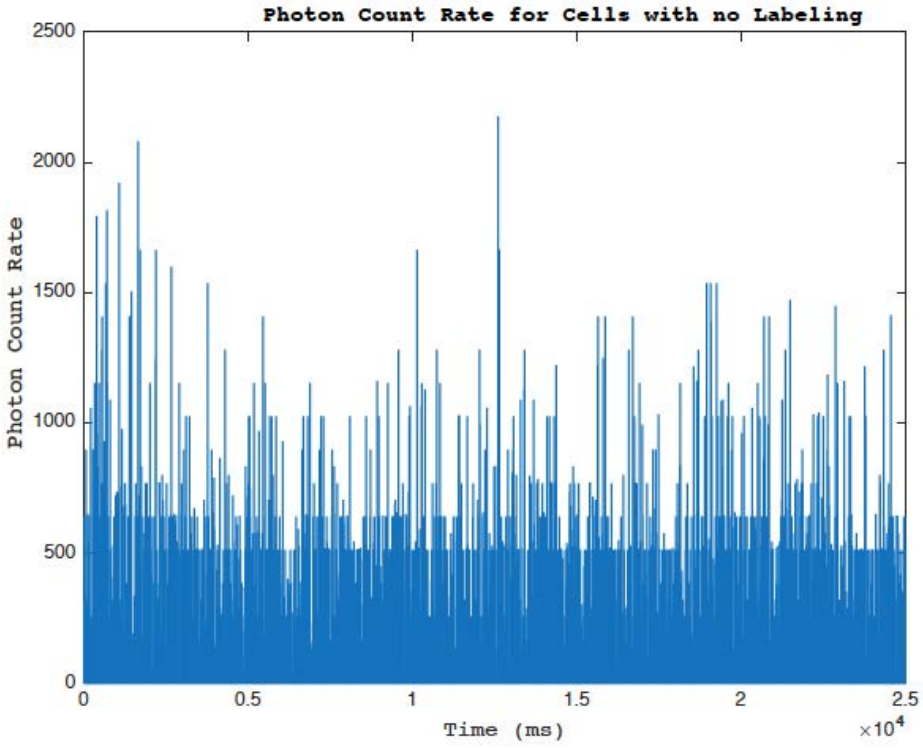

Figure 7b.
This graph displays the photon count rate of the cells with no labeling. The count rate is about 500 cps. Notice that the photon counts are above background, which means there is signal.

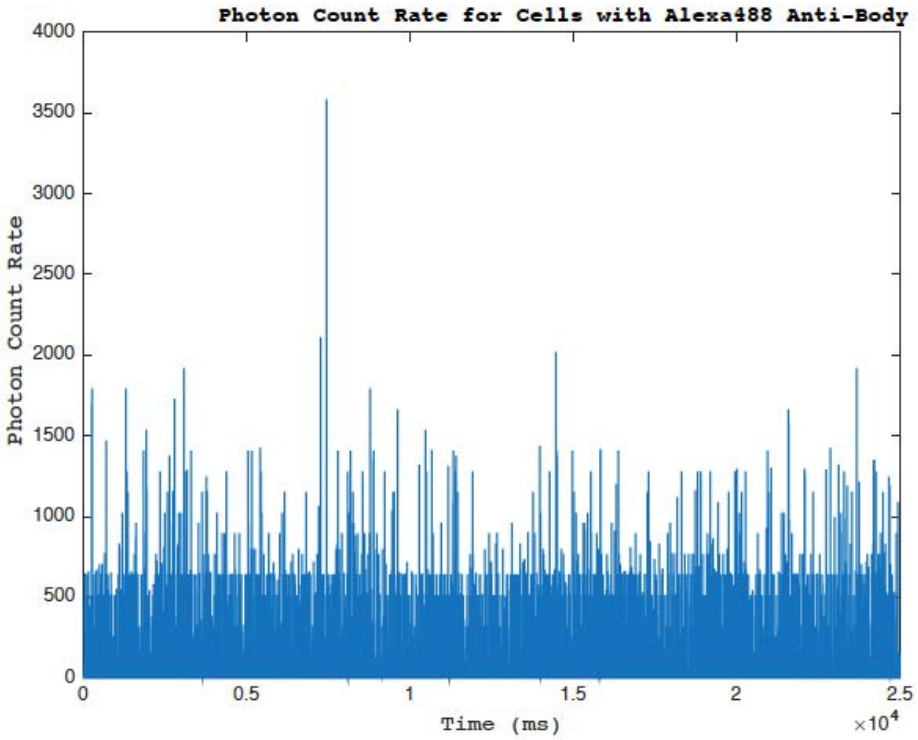

Figure 7c.
This graph of the photon count rate of the cells with the Alexa488 antibody also gives about 500 cps, the same as in Figure 7b above. We hypothesize that intrinsic cellular fluorescence dominates the signal.

As shown above, fluorescence was detected above background. However, there was no significant difference between the cells with labeling and cells without labeling. Our hypothesis is that molecules inside cells that are inherently fluorescent are dominating the signal from the alpha-4 subunit.

As stated above, the VLA-4 protein is a cell membrane protein. Thus, a technique was needed to excite fluorescence from just the cell membrane, which would eliminate any intrinsic fluorescence from inside the cell. The cells are placed in wells, and are stuck to the bottom of the well plate. This means that the cell membrane, as well as alpha-4 and beta-1, is very close to the interface between the cover slip and the aqueous medium in which the cells bathe. Total Internal Reflection Fluorescence Microscopy (TIRFM) is a technique used to only excite fluorescence near an interface. TIR is an optical phenomenon in which an incident light beam encounters a material with a lower-index medium at a high enough angle that the beam is totally reflected; in this case, there is no (real) solution for Snell's law.[4,8,9] An electromagnetic field is created in the low-index material and propagates

parallel to the interface; the electromagnetic wave is called an evanescent wave.[4,8,9] The evanescent wave does not penetrate very far into the medium and thus it is ideal for exciting fluorescent molecules that reside close to the interface.[4,8,9]

Total Internal Reflection Fluorescence Correlation Spectroscopy

When a light beam is incident on an interface with a different index of refraction, the waves fulfill the boundary condition $\vec{E}_{0I} + \vec{E}_{0R} = \vec{E}_{0T}$ (I for incident, R for reflected, and T for transmission).[9,10] Additionally, the relationship between the angle of the incident wave and the angle of the transmitted wave is given by Snell's law, $n_I \sin\theta_I = n_T \sin\theta_T$ (n_I and n_T are the indices of refraction for the medium in which the wave propagates).[9,10] The angles are measured with respect to the normal of the interface.[9,10] At a particular angle of incidence, called the critical angle, the transmitted rays are 90^0 to the normal (Figure 8).[9,10]

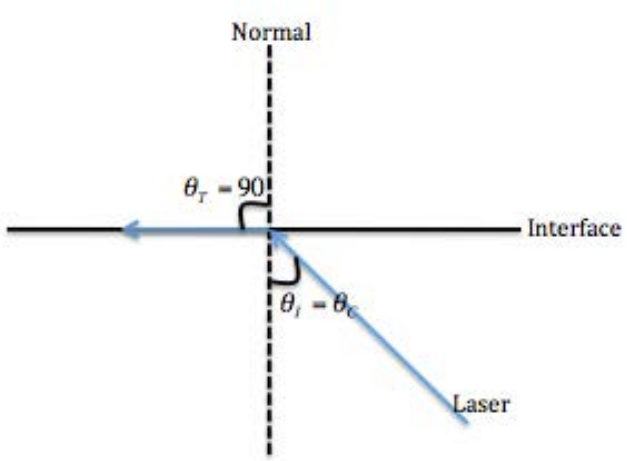

Figure 8.
Schematic of total internal reflection where, at a particular angle of incidence, called the critical angle, the transmitted rays at an interface are 90^0 to the normal.

Above the critical angle, all rays are reflected (total internal reflection) and the transmitted wave has the form of an evanescent wave.[9,10] The transmitted electric field is

$$\vec{E}_T = \vec{E}_{0T} e^{i(\vec{k}_T \cdot \vec{r} - \omega t)} \qquad (6)$$

where $\vec{k}_t \bullet \vec{r} = k_{Tx}x + k_{Ty}y$ is the wave vector dotted onto a position vector.[9] (We take the incident wave vector to lie in the x-y plane; the y direction is perpendicular to the planar interface). Again using Snell's law, and focusing only where $\sin(\theta_I) > \frac{n_T}{n_I}$, it can be shown that[9]

$$k_{Ty} = \pm ik_T\left(\frac{\sin^2\theta_I}{\left(n_T/n_I\right)^2} - 1\right) = \pm i\beta \tag{7}$$

and

$$k_{Tx} = \frac{k_T}{n_T/n_I}\sin\theta_I \tag{8}$$

The evanescent electric field is then

$$E_T = E_{0T}e^{\mp i\beta y}e^{i\left(\frac{k_T x\sin\theta_T}{n_T/n_I} - \omega t\right)} \tag{9}$$

Above the critical angle, beta is imaginary, and thus the amplitude decays (or grows) exponentially into the low index medium. From physical reasoning the positive (growing) exponential can be ignored, and the amplitude of the wave drops off exponentially with depth into the medium (in this case the boundary is the glass slide and the water or cell above it).[9] Figure 9 is a graphical representation of the evanescent wave's intensity vs. distance of penetration into the medium using n_I=1.5 (immersion oil), n_T= 1.33 (water), and λ= 488 nm.

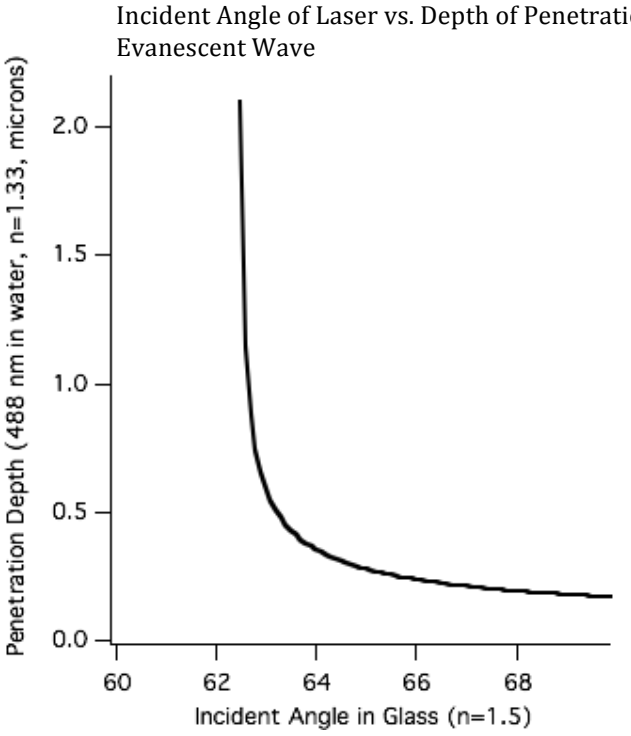

Figure 9.
Just above the critical angle, the penetration depth of the laser light will dramatically decrease, because the evanescent wave only penetrates a fraction of a micron just above the boundary.

The important conclusion to be drawn from Figure 9 is that, just above the critical angle (62.46 degrees), the penetration depth decreases significantly as the evanescent wave only travels through a fraction of a micron just above the boundary. Thus, in order to confirm TIR in our experiments, the same characteristic must be displayed.

TIR-FCS using a Nikon Inverted Microscope Eclipse TE200

A new optical set up was created that would allow for TIR with confocal alignment in a microscope, displayed in Figure 10 (see procedure in Appendix 1.2).

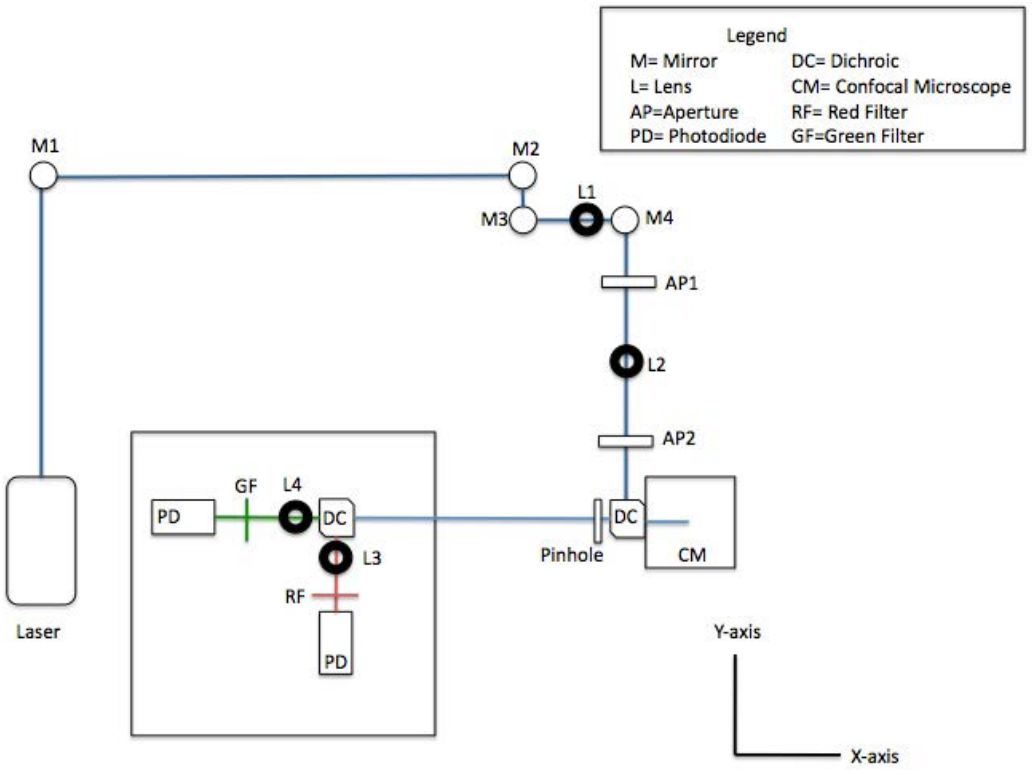

Figure 10. Optical Set Up for FCS with TIR using a confocal microscope

The key with this set up is that a mirror must be placed on a translation stage in such a way that when the mirror angle is changed by rotation, it will change the angle of incidence of the laser in the objective of the microscope, *without moving the laser spot* in the FOV. Consideration of the objective numerical aperture was also taken into consideration before beginning the experiments. The equation for the numerical aperture (NA) is: $NA = n_T \sin\theta_T$. The maximum angle reached by θ_T is 90^0 (just before TIR). Using n_T= 1.33, this means an NA=1.33 is the threshold for obtaining TIR. Given the finite size of the illuminating laser beam, we must have an NA greater than 1.33. The NA for the Zeiss objective used is 1.4 (Appendix 3) and thus TIR should be possible using this objective.

After the initial set up was completed, angle vs. intensity measurements were made to determine if TIRFM would be successful using the microscope. First, a glass hemisphere was placed on the objective (Appendix 3) of the microscope with oil immersion between the hemisphere and the objective, and a protractor was placed next to the hemisphere. The angle of the rotating mirror was changed slightly so as

to affect the angle of incidence of the laser at the objective. Measurements were taken for the angle of the rotating mirror and the corresponding angle of incidence of the laser on the objective, as shown in Figure 11.

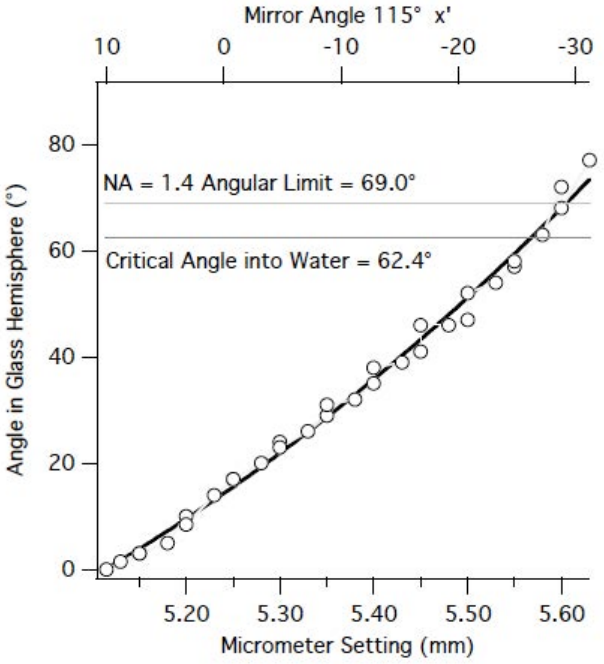

Figure 11.
This plot shows the relationship between the pivot mirror's micrometer setting and angle with respect to the optical axis, and the output angle of the laser in the glass hemisphere on the microscope. The micrometer has a translational movement that controls the angle of the mirror. The bottom axis denotes the translational movement, and the top axis denotes the angle of the mirror as a function of micrometer setting. Note that the calculated critical angle is smaller than the angular limit, thus it is believed that TIR can be achieved.

Using Snell's law, and, again, the indices of refraction for glass and water as 1.5 and 1.33, respectively, the critical angle was determined to be 62.46 degrees.

Intensity vs. illumination angle was then measured for a fluorescent solution, to look for the sharp drop in intensity at the critical angle that was expected (Figure 9, above). Many different attempts at taking angle vs. intensity measurements were made; however, none gave consistent results. One problem that arose was that the reflected light either off the sample or other object was too great to determine when TIR had been reached. (Even though there is a barrier filter to remove laser light, a strong back reflection will give some small transmission through this filter, which could overwhelm the fluorescence signal. In order to correct for this, it was determined that black electrical tape could be placed on the back of the objective to block the reflected beam. The laser beam enters the objective, hits the sample, and then exits the objective. The electrical tape was placed so that it was symmetric to

where the laser light entered the objective, thus blocking the reflected light, as displayed in Figure 12.

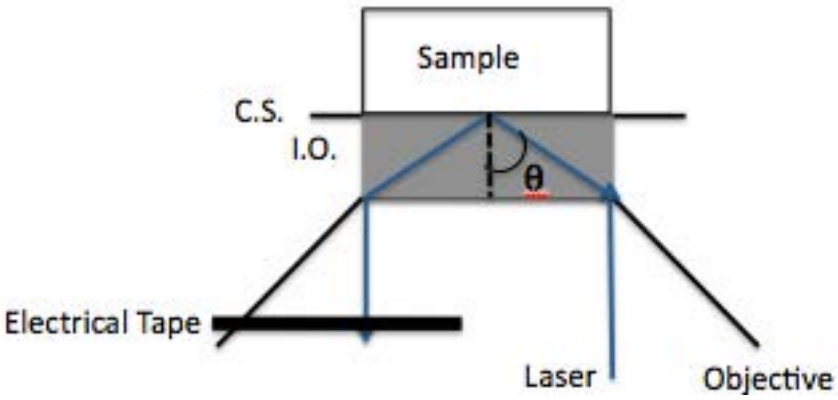

Figure 12.
Schematic of the laser path as it hits the objective lens, is redirected to hit the sample, then is reflected back through the objective at a position symmetric to where it entered the objective. (In this cartoon, the objective is modeled as a thin lens at the bottom of the gray region.) Electrical tape was placed at a position symmetrically from the incident laser so as the block the reflected laser beam. (C.S. : cover slip, I.O. : immersion oil.)

With the electrical tape blocking the reflected light it was expected that the measured intensity from the sample would initially drop when the laser hit the electrical tape, and then another drop in intensity would correspond to TIR. Unfortunately, this was not observed. An initial drop in intensity was measured, however a significant second drop was not observed, and TIR could not be confirmed. It is thought that this could have been a result of the Gaussian nature of the laser beam. Since positions in the back focal plane of the objective give different incident angles at the sample, the tail of the Gaussian laser distribution can impinge on the sample below the critical angle, even if the center of the beam is well above the critical angle. (In addition, some of the reflected Gaussian beam must necessarily miss the blocking tape. This is likely to be less important, since there is a barrier filter). Another issue, which arose throughout the measurement of the TIR angle, is diffraction of the laser beam. Above the critical angle, the laser diffracts considerably, and it is difficult to precisely measure the angle of the incident laser beam. This diffraction could lead to the possible error in measurement above TIR because it would hide the expected drop in intensity. With the above issues, no reliable, reproducible measurements were taken and a simpler microscope was

built using only an objective and a glass hemisphere in hopes that it would eliminate the problems with diffraction and reflection.

TIR-FCS Using a Glass Hemisphere and Mitutoyo Objective

After TIR-FCS was not successful using the confocal microscope, it was decided that only a glass hemisphere, Mitutoyo objective (Appendix 3), and photodiode would be used instead, as it was a simpler set up and it could potentially eliminate the problems of reflection and diffraction. First, a check of the index of refraction of the glass hemisphere was made. The hemisphere was placed on a rotation stage on the middle of the axis of rotation, and the laser was directed toward the center of the hemisphere. As the hemisphere rotated, measurements of the incident angle and transmitted angle were recorded. Again, using Snell's law, $n_a \sin\theta_I = n_g \sin\theta_T$ (n_a=1, the index of refraction for air, n_g is the index of refraction for the glass hemisphere, θ_I = incident angle of the laser on the hemisphere as measured from the normal, and θ_T = transmitted angle as measured from the normal), it is easily seen that $n_g = \frac{\sin\theta_I}{\sin\theta_T}$. Making substitutions for $x = \sin\theta_I$ and $y = \sin\theta_T$, this is easily translated into a linear equation, with n_g^{-1} as the slope. Figure 13 shows the plot for $y = \frac{1}{n_g}x$.

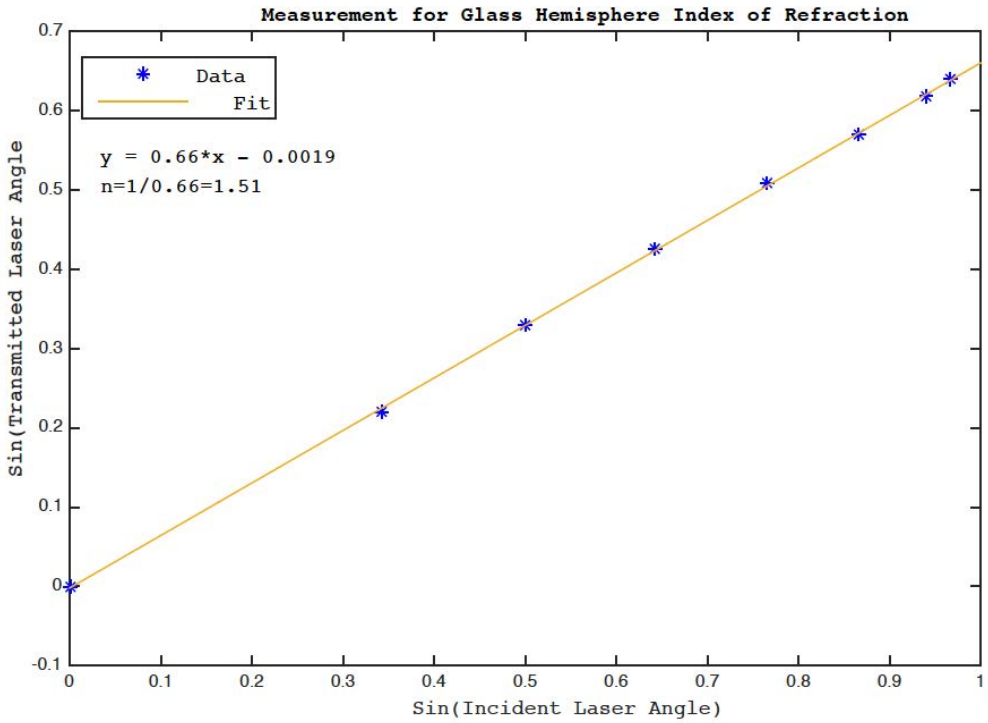

Figure 13.
This graph clearly shows the linearity between the $\sin(\theta_I)$ and $\sin(\theta_T)$, thus providing the index of refraction for the glass hemisphere to be 1.51.

With the index of refraction for the glass hemisphere confirmed to be 1.51, a new optical apparatus was created (see Appendix 1.3 and Figure 14 below). The set-up was arranged so that the angle of incidence could be varied through a small range of angles around the TIR angle, by simply rotating the hemisphere.

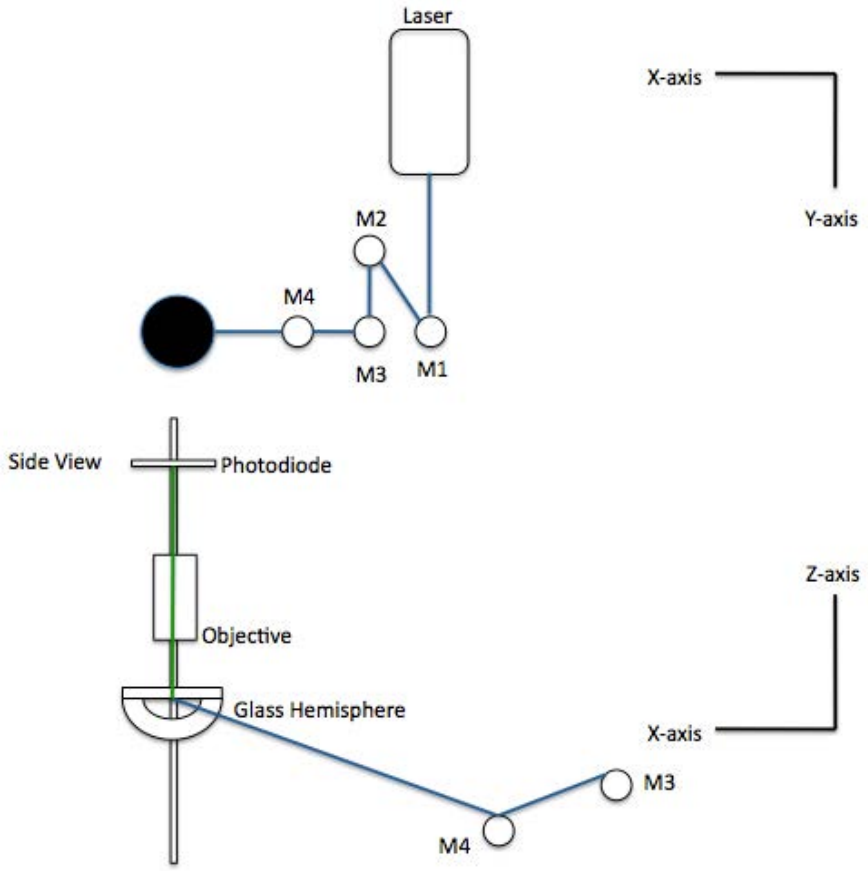

Figure 14.
Optical Set Up for FCS with TIR using a glass hemisphere and objective.

For these measurements, a lock-in amplifier and beam chopper were used. First, a background measurement was taken and was found to be 0.0005 mV on a lock-in amplifier. It is important to take a background measurement to ensure that the signal received from a fluorescent source is detected. Next, a thin fluorescent film was used to determine whether the signal had any artifactual angular dependence. (This could arise from imperfect alignment, if the illuminated region moves slightly as the hemisphere is rotated, for example). With a fluorescent film, the amount of fluorescence is essentially independent of the angle of incidence of the laser. Figure 15 shows the relationship between the angle of the fluorescent film and the intensity measurement. The fluorescent film is not completely uniform, so three sets of data were taken and averaged to get an average intensity measured across the film.

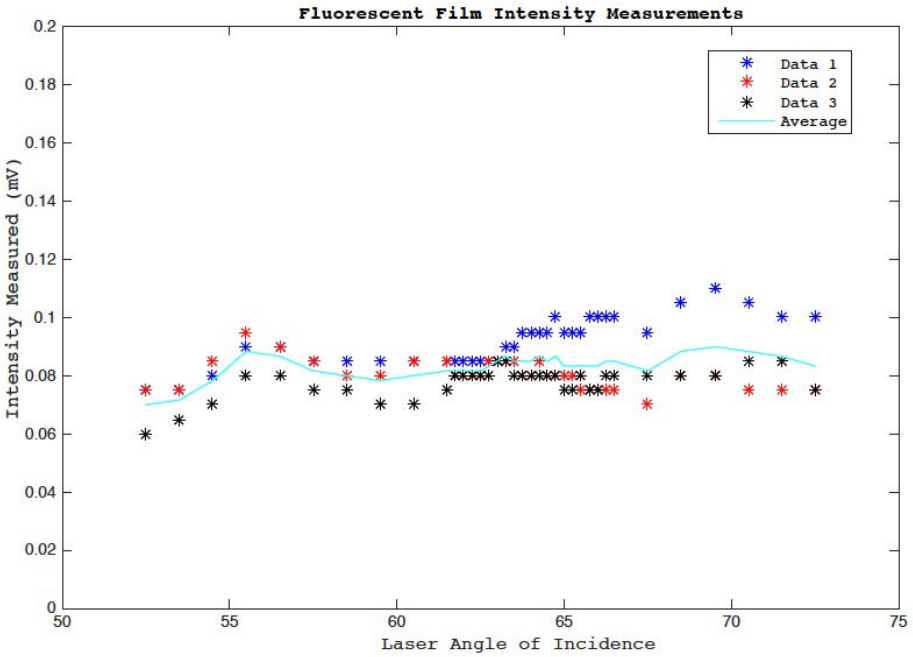

Figure 15.
The difference in the intensity measurements taken from the fluorescent film do not change appreciably, especially around the critical angle. Thus this set up will give reliable and consistent measurements.

The above data show that while there are some slight changes in intensity it is not appreciable enough to invalidate the data. Furthermore, at the critical angle (plus or minus a couple degrees) intensity measurements were consistent. Finally, a fluorescent solution was made (see Appendix 1.4) to take intensity measurements for TIR. Data was collected on the fluorescence intensity vs. the angle of incidence, displayed in Figure 16a.

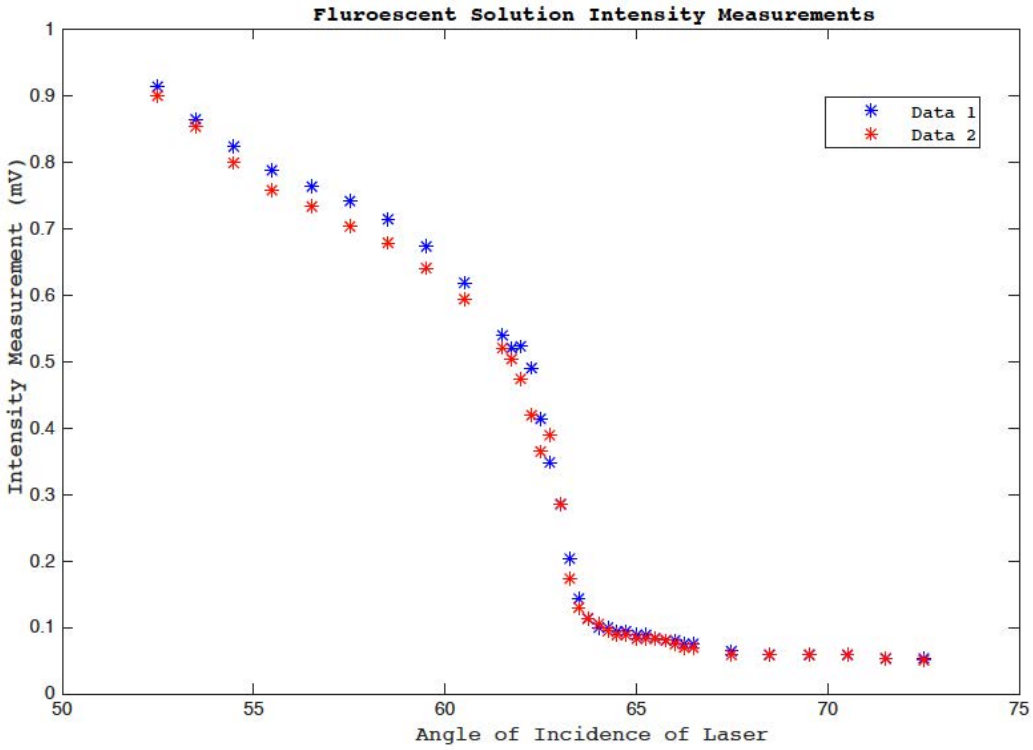

Figure 16a. The fluorescence intensity measured from an aqueous solution of dye, plotted as a function of the incident laser angle. Note the dramatic drop in intensity around the critical angle.

This data displays the expected decrease in intensity right around the critical angle. To model the fluorescence intensity, we find the intensity in the evanescent wave as a function of distance from the interface (y) and integrate from the interface to infinity. (The fluorescence intensity is proportional to the illumination intensity, for a one-photon absorption process). Squaring and integrating $E_T = E_{0T}e^{\mp i\beta y}$ (from equation (9), β imaginary) from zero to infinity gives $I = \frac{I_0}{2\beta}$, which is proportional to the penetration depth. The data in Figure 16a was fit to $I = \frac{I_0}{2\beta}$ with I_0 as the only free parameter using the method of least squares. The result of this fit is shown in Figure 16b.

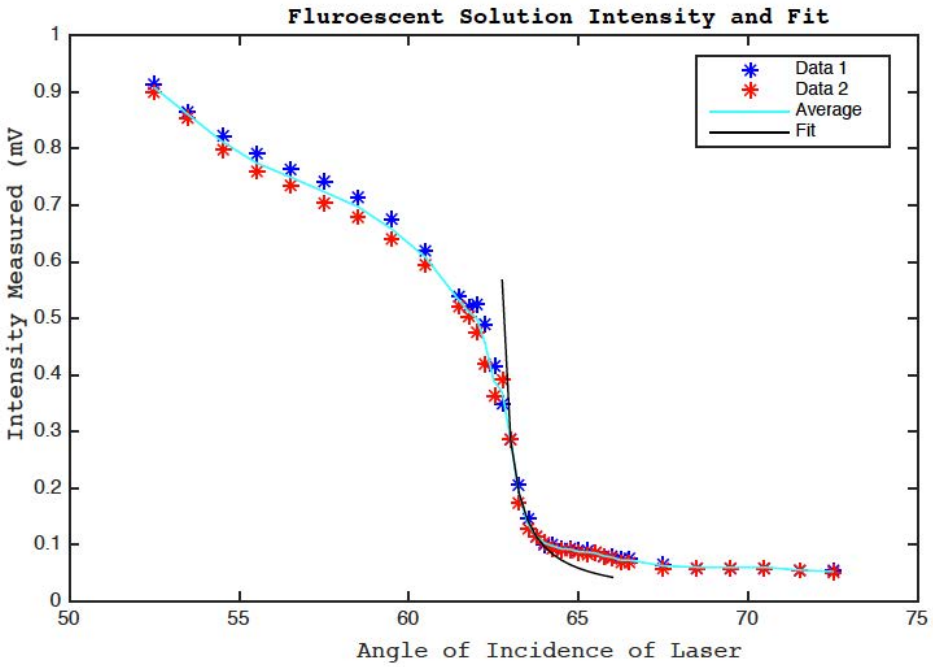

Figure 16b.
This figure shows the data taken using the fluorescent solution, an average of the data, and a fit to the average. Around the critical angle there is a dramatic drop in intensity, matching the theory that the evanescent wave's penetration depth is only a fraction of a micron just above the critical angle, and thus a drop in intensity is expected.

These plots clearly show the expected drop in intensity around the critical angle, which confirms that TIR is achieved with this optical apparatus, and it can be used for reliable, consistent measurements using live cells.

Conclusions and Future Work

Now that TIR has been confirmed using the simpler TIR-FCS apparatus, it would be beneficial to understand why TIR-FCS was not successful using the microscope. To test the Gaussian nature of the beam, and possibly correct for it, the size of the beam diameter could be decreased using a beam expander. Additionally, using a beam expander to reduce the size of the laser, along with covering a certain area of the objective with electrical tape, could more fully block out any of the reflected beam and also ensure that more of the beam is incident on the glass-water interface above the critical angle. Next, it would be constructive to understand why the laser diffracts above the critical angle, even though theoretically it should be able to reach an angle above the critical angle. One hypothesis is that one of the lenses or another object inside the microscope is affecting the incidence of the laser at the objective. After this is determined, depending on the source of diffraction, a beam expander could again help solve this issue, as a smaller beam diameter may hit the diffraction source at a higher incident angle, which would allow for TIR. Another possibility is to turn the wells that the cells are held in upside down on the microscope objective, place a hemisphere on top of the wells, and then direct a laser through the hemisphere to excited the cells in TIR. If none of the above solutions help solve the problem, the glass hemisphere and objective apparatus can still be used for measurements with live cells. In this case, the set up must be modified for two-channel TIR-FCS. Whether using the microscope or the glass hemisphere, the correlation between alpha-4 and beta-1 will need to be confirmed using a TIR-FCS apparatus. Finally, it is hoped that the two sub-units will be shown to dissociate after the introduction of Thioridazine to the system.

Acknowledgements

I would like to thank, first and foremost, Dr. Thomas for being my advisor for the last two years. His mentorship and teaching helped me fully understand not only the theories behind my research but also what it takes to be a research scientist. Next I would like to thank Samantha Schwartz for teaching me about ICS as well as basic techniques used in a lab such as cell microscopy. I would also like to thank Dr. Lidke for letting me use his ICS-TIR optics at the beginning of this project. A big thanks also goes to Dr. Alexandre Chigaev and Dr. Yelena Smagley for preparation of the fluorescent cells. I would also like to thank the College of Arts and Sciences and those on the committee for the Frank O. and Sadie M. Lane Scholarship, as this scholarship was what allowed me to do this research as an undergraduate. Finally, I would like to thank the Physics and Astronomy Undergraduate Committee for reviewing my thesis and giving me the opportunity to present my work.

References

1. A. Chigaev, Y.W.u, D. B. Williams, Y. Smagley, and L. A. Sklar, Journal of Biological Chemistry, **286**(7), 5455-5463 (2011)
2. H. Yusuf-Makagiansar, M.E. Anderson, T.V. Yakovleva, J.S. Murray, and T.J. Siahaan, Medicinal Research Reviews, **22**(2), 146-167 (2002).
3. J. Ries and P. Schwille, Bioessays **34**, 361-368 (2012).
4. R. Rigler and E.S. Elson, *Fluorescence Correlation Spectroscopy* (Springer, New York, 1965), Chap. 8, p. 165-168, Chap. 9, p. 187-188, Chap. 17, p. 360-364.
5. K. Kneipp, R. Aroca, H. Kneipp, and E. Wentrup-Byrne, *New Approaches in Biomedical Spectroscopy* (Oxford University Press, 2007), Chap 17, p. 267-269.
6. T. E. Starr and N.L. Thompson, Biophysical Journal, **80**, 1575-1584 (2001).
7. J. Krieger, K. Toth, and J. Langowski, German Cancer Research Center, Practical Course in Biophysics: Fluorescence Correlation Spectroscopy, p. 3-11.
8. A. Chigaev and Y. Smagley, (private communication).
9. T. Ursell, California Institute of Technology, Biological Physics Laboratory: *Diffusion of Solid Particles Confined in a Viscous Fluid* (2005).
10. N. L. Thompson and B. L. Steele, Nature Protocols, **2,** 4 (2007).
11. E. Hecht, *Optics* (Addison Wesley, San Francisco, 2002), Ed. 4, p. 125.
12. H. Young and R. Freedman, *University Physics with Modern Physics* (Addison-Wesley, San Francisco, 2012), Ed. 13, p. 1083-1089.
13. B. Hebert, S. Constantino, and P. W. Wiseman, Biophysical Journal, **88**, p. 3601-3614 (2005).
14. N. O. Petersen, P. L. Hoddelius, P. W. Wiseman, O. Seger, and K. E. Magnusson, Biophysical Journal, **65,** p. 1135-1146 (1993).
15. P. W. Wiseman, C. M. Brown, D. J. Webb, B. Hebert, N. L. Johnson, J. A. Squier, M. H. Ellisman, and A. F. Horwitz, Journal of Cell Science, **117**, p. 5521-5534 (2004).
16. M. W. Davidson, Nikon Microscopy, *Numerical Aperture Light Cones* (2013)

Appendix 1

1. Optical Set Up for FCS Without TIR

Throughout this procedure, use Figure 1 as a reference.

0. A dichroic mirror is positioned next to the side port of the microscope that brings the laser from the back of the table into the microscope. The dichroic reflects 488 nm and passes ≥ 500 nm. The laser is approximately 488 nm so it is reflected into the microscope. The magnification of the image coming out of the microscope is 61X, and a black line on the table marks the image plane.

1. Determine the optical axis.
    a. One aperture, AP2, will be used to determine the optical axis (which is also the X-axis), which will then be used later to align the laser. Take AP2 and place it in line with the dichroic mirror, approximately on the optical axis.
    b. In a very dark room, and using either the Edmund Grating or removing the objective and placing an aperture on the objective turrets, turn the condenser light up to full intensity. If using the Edmund Grating, find a spot or letter and center it in the cross hairs of the microscope. The shape that you use should be easily identified as the center of the field of view.
    c. Using back projection, place AP2 as close to the focal plane as possible.
    d. Now align the center of AP2 with the center of the back projected image.
2. Align the laser through the optical axis.
    a. Two mirrors will be used for this process. Determine the height of the center of AP2, and place the center of one of the mirrors at this height and along the optical axis (this will be mirror 2, M2).
    b. Mirror 1, M1, should be placed directly in line with the laser coming out of the optical cavity, the laser should hit the approximate center of M1. With M2 placed in line with AP2, and the two mirrors be in line with each other along the y-direction. The laser will come out, hit M1, and be re-directed to hit M2, which will then redirect it again to go through the center of AP2 and into the microscope.
    c. Adjust M1 and M2 as necessary so that the mirror goes straight through the center of AP2.
3. Check the laser divergence out of the microscope
    a. Replace the aperture or Edmund Grating with an objective. Check that the laser diverges uniformly out of the objective. It should also focus to a small spot in the center of the field of view, when viewed using the Edmund Grating. **Caution: attenuate the laser beam! Always check with your hand that the laser light is not emerging from the eyepieces before looking in the microscope.**

   b. To improve the alignment, M2 can be used to better position the spot in the field of view, and the dichroic mirror can be adjusted to get uniform divergence out of the objective.
4. Placement of Lens 2 (L2) and the back focal plane aperture (AP1)
   a. Find the focal length of the lens that will be used to focus an image in the back image plane.
   b. The lens equation is used to determine the placement of L2 and AP1. AP1 is the image distance of L2, and the object distance is the distance between L2 and the FOV in the microscope.
   c. Calculate and determine the placement for L2 so that it is centered on the optical axis.
   d. Next determine the placement for AP1. The best way to do this is to place L2 centered on the optical axis, and find where the image flips behind L2. Where the image flips is where AP1 should be placed. Next, remove L2 and align AP1 with the back projection (similar as in step 1). Then, similar to step 2, reposition M1 and M2 so that the laser goes straight through the center of AP1 and AP2. Replace L2, and make sure the laser still goes straight through the center of AP1 and AP2.
5. Placement of L1
   a. Find the focal length of the lens that will be used to focus the laser at AP1.
   b. Place L1 at this distance from AP1, as in Figure 1.
6. Align the Detection Pinhole
   a. An analog photodiode should be placed in line with the light that comes out of the side of the microscope. Place the photodiode on a translation stage and move it until it reads a maximum signal from the sample.
   b. Place a 100-micron pinhole as close to the dichroic as possible. This should also be on a translation stage that can go in both the X and Z directions. Adjust the position of the pinhole until, again, a maximum signal is read on the photodiode.
7. Align the Digital Photodiodes
   a. Remove the analog photodiode and add a second dichroic mirror in its place.
   b. Add lenses 3 and 4, corresponding to each path of the second dichroic. The focal length of these lenses should be measured and the size of the spot that hits each digital photodiode using the chosen lenses should be calculated so that the spot size is smaller than the photodiode. Thus, the photodiodes (on translation stages again) are placed at the focal length of each lens.
   c. Maximize the signals received on each photodiode by moving them in the X, Y, or Z directions as needed.
   d. Appropriately place a filter at each outgoing channel of the second dichroic so that only a green signal will reach one of the photodiodes, and only a red signal reaches the other.
8. Take 2 channel fluorescent measurements!

Figure 1. Optical Set Up for FCS without TIR

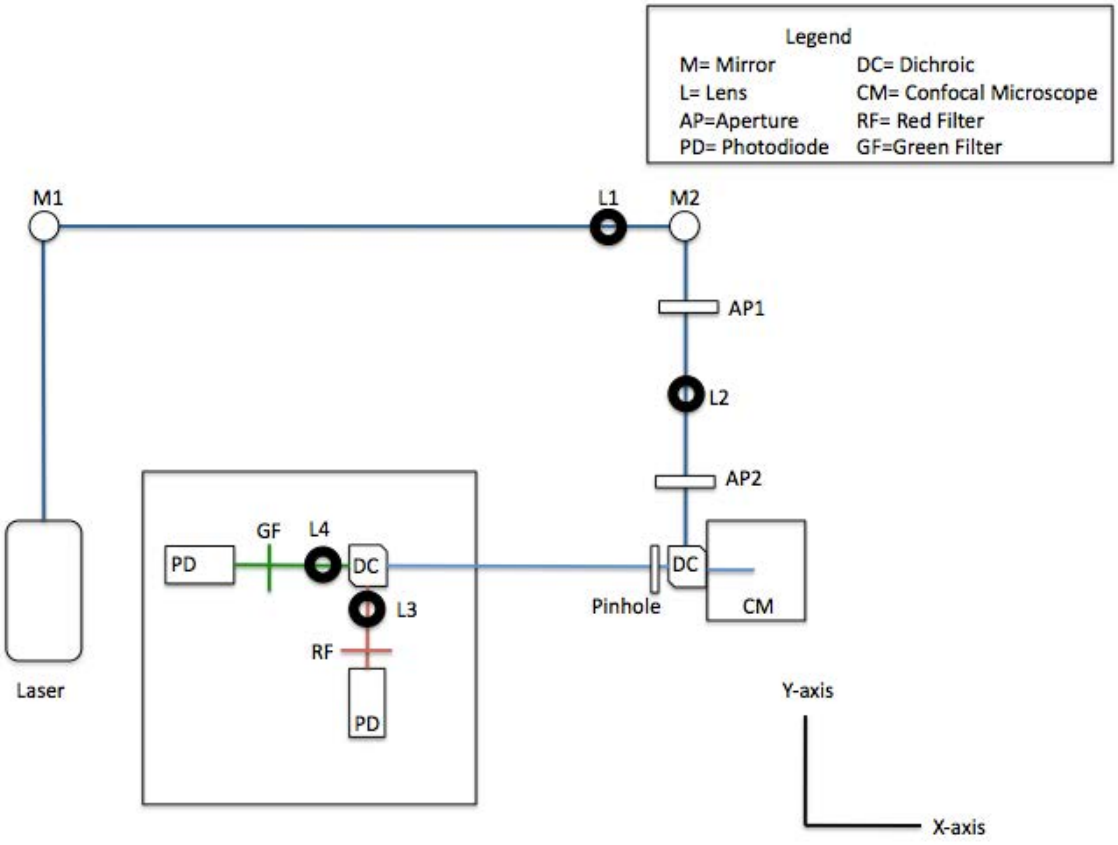

2. Optical Set Up for TIR-FCS using a Nikon Inverted Microscope Eclipse TE200

Throughout this procedure, use Figure 2 as a reference.

0. A dichroic mirror is positioned next to the side port of the microscope that brings the laser from the back of the table into the microscope. The dichroic reflects 488 nm and passes ≥ 500 nm. The laser is approximately 488 nm so it is reflected into the microscope. The magnification of the image coming out of the microscope is 61X, and a black line on the table marks the image plane.

1. Determine the optical axis.
    a. One aperture, AP2, will be used to determine the optical axis (which is also the X-axis), which will then be used later to align the laser. Take AP2 and place it in line with the dichroic mirror, approximately on the optical axis.
    b. In a very dark room, and using either the Edmund Grating or removing the objective and placing an aperture on the objective turrets, turn the condenser light up to full intensity. If using the Edmund Grating, find a spot or letter and center it in the cross hairs of the microscope. The shape that you use should be easily identified as the center of the field of view.
    c. Using back projection, place AP2 as close to the focal plane as possible.
    d. Now align the center of AP2 with the center of the back projected image.
2. Align the laser through the optical axis.
    a. Two mirrors will be used for this process. Determine the height of the center of AP2, and place the center of one of the mirrors at this height and along the optical axis (this will be mirror 2, M2).
    b. Mirror 1, M1, should be placed directly in line with the laser coming out of the optical cavity, the laser should hit the approximate center of M1. With M2 placed in line with AP2, and the two mirrors be in line with each other along the y-direction. The laser will come out, hit M1, and be re-directed to hit M2, which will then redirect it again to go through the center of AP2 and into the microscope.
    c. Adjust M1 and M2 as necessary so that the mirror goes straight through the center of AP2.
3. Check the laser divergence out of the microscope
    a. Replace the aperture or Edmund Grating with an objective. Check that the laser diverges uniformly out of the objective. It should also focus to a small spot in the center of the field of view, when viewed using the Edmund Grating. **Caution: attenuate the laser beam! Always check with your hand that the laser light is not emerging from the eyepieces before looking in the microscope.**
    b. To improve the alignment, M2 can be used to better position the spot in the field of view, and the dichroic mirror can be adjusted to get uniform divergence out of the objective.
4. Placement of Lens 2 (L2) and the back focal plane aperture (AP1)

   a. Find the focal length of the lens that will be used to focus the back image plane.
   b. There are two lens equations that come into play with the placement of L2 and AP1. The first lens equation involves AP1 as the image distance of L2, and the object distance is the distance between L2 and the FOV in the microscope. The second involves AP2 as the image distance of L2 and the pivot mirror (M4) as the object distance of L2 (placing M4 doesn't come until step 5, so just mark it on the table for now).
   c. Calculate the placement for L2 so that it is centered on the optical axis, AP2 is the image distance of L2 with the object distance being M4. Next, determine the position of AP1. The best way to do this is to place L2 centered on the optical axis, and find where the image flips behind L2. Where the image flips is where AP1 should be placed. Next, remove L2 and align AP1 with the back projection (similar as in step 1). Then, similar to step 2, reposition M1 and M2 so that the laser goes straight through the center of AP1 and AP2. Replace L2, and make sure the laser still goes straight through the centers of AP1 and AP2.
5. Approximate placement of mirrors 1, 2, 3, and the pivot mirror
   a. In the final placement of mirrors 1, 2, 3, and the pivot mirror (M1, M2, M3, and M4, respectively), the laser will hit M1, be redirected to M2 along the Y-direction, which redirects it to M3 along the X-direction, and finally to M4, again along the Y-direction. M4 will be placed on a translation stage TS2, a platform P1, another translation stage (TS2), and then on a rotation stage (RS1). M3 will also be place on a translation stage (TS3), which is on P1, in such a way that TS3 can move along the Y-direction, similar to M4 but in the opposite direction and on the opposite side of P1. Finally, a lens, L1, will also be placed on P1, and on a translation stage TS4. Thus, P1 must be large enough to hold TS2-4, L1, and allow everything to move freely. This step is an approximate placement procedure, and all placements will be finalized in step 6. The placement of L1 will not be determined until step 8.
   b. Place P1 around the center of TS1, and in such a way that TS1's micrometer can be easily accessed. TS1 should be directed so that it translates along the Y-direction.
   c. Place TS2 on top of P1, and RS1 on TS2 in such a way that M4 can be aligned along the optical axis. The height of M4 should be approximately the same as the center height of AP2, so measure accordingly and place a mirror that fits that parameter.
   d. Now determine the approximate distance/placement of M3 from M4 (this will change slightly in the next few steps). M3 should be along the same Y-axis as M4.
   e. Place M2 so that when the laser is directed from M2 to M3, it is parallel to the X-axis.

    f. At this point, align M1 with M2 and adjust so that when the laser hits M1, it is redirected to M2, which then redirects the laser to M3. Again, the laser, going from M2 to M3, should be parallel to the X-axis. Furthermore, the height of the laser at M2 should be the same as the height of the laser at M3, which should be the same as the height of the center of M4. Make adjustment in the tilt/ pivot of M1 and M2 to make this possible.

6. Final placement of mirrors 1, 2, and 3
    a. In the final placement of mirrors 1, 2, and 3, the laser will hit M1, be redirected to M2 along the Y-direction, which redirects it to M3 along the X-direction, and finally to M4 again along the Y-direction, and then the laser should go straight through the centers of AP1/2.
    b. Make adjustments to M3 by using the translation stage, and the tilt/ pivot of M3 to make this possible.
7. Check the laser in the field of view of the microscope
    a. The laser should still diverge uniformly coming through the microscope, and it should be at the center of the field of view when viewed using the Edmund Grating. If it is not, minor adjustments to M4 can be made so that it does.
8. Final placement of M4 and everything on P1
    a. When M4 is on the exact center of the optical axis and the object distance of L2, then as M4 is rotated, the position of the laser spot will not move at AP2. Adjust P1 by moving it either closer or farther from AP1 as needed, and check the alignment of M4 by rotating it. When the laser spot doesn't move from the center of AP2, then M4 is in the correct position.
9. Placement of L1
    a. Determine the focal length of L1.
    b. The focal point of L1 should be at AP2, so place L1 accordingly.
    c. Again, adjust L1 so that the laser remains in the center of the FOV, as before.
10. Confirm TIRF
    a. Place the glass hemisphere on top of the microscope and set up a protractor at the center of the hemisphere so that angle measurements of the laser coming out of the microscope can be made.
    b. Using the micrometer settings on RS1, rotate M4 every 2-3 micrometers.
    c. Measure the angle, ø, that comes out of the microscope and take $\Omega=90-ø$ as the outgoing angle of the laser. Do this one to two more times to get an average.
    d. Graph Ω vs. micrometer setting as a reference.
    e. Place a lens, L3, with a short focal length at the image plane of the microscope (the image plane on the side of the dichroic mirror), and in such a way that the laser spot hits L3 at the center. Also put a photodiode on a translation stage moving in the X-direction, at the focal length of L3. Adjust the photodiode's position until a maximum

signal is read. The size of the photodiode should be greater than the diameter of the laser, and, in case M4 isn't precisely on the optical axis and moves *slightly* in the image plane (no more than the radius of the laser spot), L3 will redirect the laser to hit the photodiode in the center. This ensures that the entire signal is recorded.

f. Starting at Ω=0 degrees, rotate M4 approximately 10 microns, and record the movement of the laser spot. Repeat until Ω is past the 65-degree mark. If the laser spot moves more than L3 can redirect it to the photodiode, M4 is not correctly positioned.
    i. What to do if M4 is not correctly positioned
        1. If the laser does not hit M4 in the exact middle, or if it is not at the image distance position of L2, then the spot size will move too much in the image plane of the microscope for the photodiode to record all of the intensity.
        2. First check that the laser hits the exact center of M4, and that the mirror is in the exact middle of rotation. If the first requirement is not met, change the position of M3. If the latter requirement is not met change the position of M4. Manipulating TS2 and TS3 can change the positions of M3 and M4. Furthermore, continually ensure that the laser goes straight through AP1/2 and is at the center of the field of view.
        3. Recheck the movement of the laser spot on the photodiode as in step 10 f. above. If the laser no longer moves, skip to step 10 g. If it still moves too much check the position of M4 in relation to L2. If M4 is not at the image distance of L2, then move TS1 accordingly. Then, again, check the movement of the laser until the laser spot no longer moves more than the length of its own radius.
g. Create a fluorescent solution that will be the sample used in the following steps. This project used a Calcein solution with a concentration of .1 g/L and a pH of 7.2 (see Appendix 1.4).
h. In a very dark room, starting at Ω=0 degrees take measurements of intensity vs. micrometer setting. Note: the recommendation is to take measurements every 3 microns until 57 degrees, then take measurements every 2 microns. Total Internal Reflection should occur between Ω=62.5-65 degrees, and the intensity of the sample's signal will drop approximately by a factor of 5.
i. Graph intensity vs. micrometer setting, and then graph intensity vs. Ω. Again, the intensity should drop by a factor of 5 when in TIRF, and this should be reflected in the graph.

11. Set up for FCS

a. First, maximize the sample's signal on the photodiode. This is done, again, with the laser at Ω=0, and moving the photodiode until it reads a maximum signal from the sample.
b. Place a 100 micron pinhole just on the other side of L3. Two translation stages are necessary to adjust the pinhole position in both the X and Z directions. Maximize the sample's signal by adjusting the pinhole position in both the X and Z directions.
c. Remove the photodiode and add a second dichroic mirror in its place.
d. Add lenses L4 and L5, corresponding to each path of the second dichroic. The focal length of these lenses should be measured and the size of the spot that hits each photodiode using the chosen lenses should be calculated so that the spot size is smaller than the photodiode. Photodiodes (on translation stages again) are placed at the focal length of each lens.
e. Maximize the signal received on each photodiode by adjusting each in either the X, Y, or Z direction as necessary.
f. Appropriately place a filter at each outgoing channel of the second dichroic so that only a green signal will reach one of the photodiodes, and only a red signal reaches the other.

12. Take 2 channel fluorescent measurements!

Figure 2. Optical Set Up for FCS with TIR using a confocal microscope

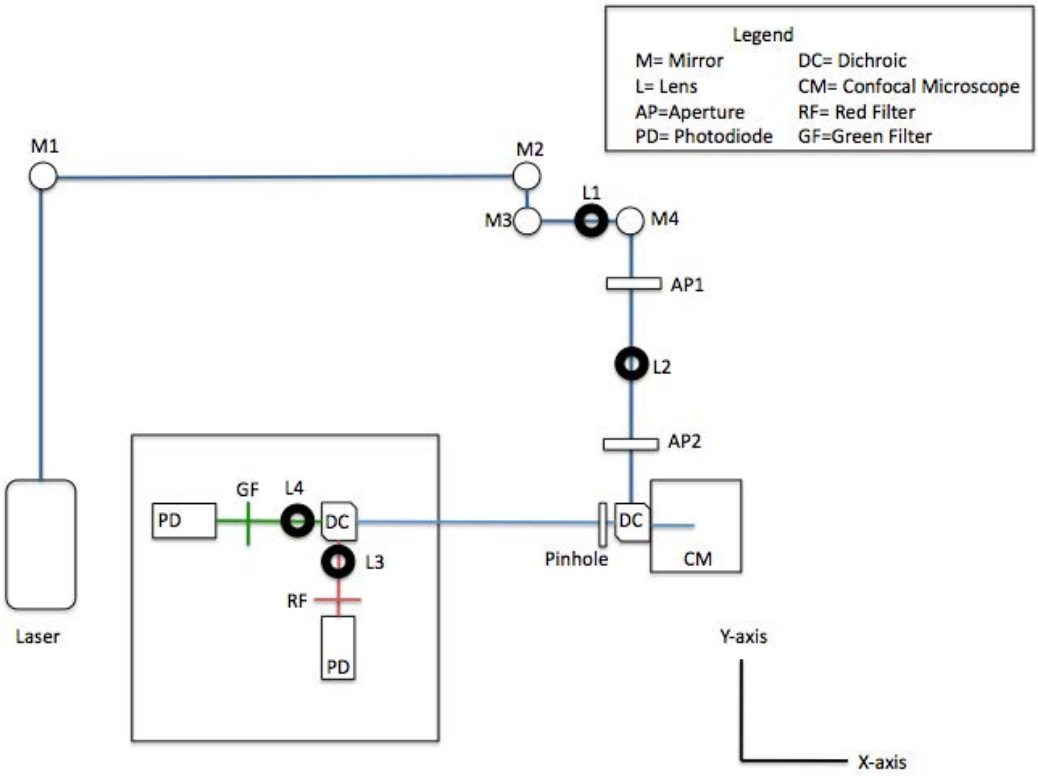

3. Optical Set Up for TIR-FCS using only the Hemisphere and Objective

Throughout this procedure, use Figure 3 as a reference.

1. Placement for the Glass Hemisphere
    a. Place the glass hemisphere on a rotation stage so that the center of the flat side is at the center of the axis of rotation. Then, it should also be placed between 15 and 20 cm above the table.
2. Placement of the Objective and Photodiode
    a. An objective should be placed above the glass hemisphere, and a photodiode above that. In this project a Mitutoyo 20X objective was used (Appendix 3). These three should be positioned so that the focus of the objective is on the glass hemisphere, and the photodiode is placed at 'infinity'.
3. Placement of M4
    a. M4 will be used to direct the laser's angle of incidence on the glass hemisphere. The critical angle necessary to create TIRF using immersion oil and water is 62.5 degrees. Thus, the laser must hit the edge of the glass hemisphere at around 62.5 degrees. Using the Pythagorean Theorem, determine the appropriate distance that M4 must be placed to achieve an angle of incidence of approximately 62.5 degrees.
4. Direct the Laser to M4
    a. Using a set of 1 or 3 mirrors, direct the laser out of the optical cavity so that it hits M4 and is redirected to the glass hemisphere at, of course, the critical angle.
5. Take measurements of angle vs. intensity and confirm TIR using the glass hemisphere

Figure 3. Optical Set Up for FCS with TIR using a glass hemisphere and objective.

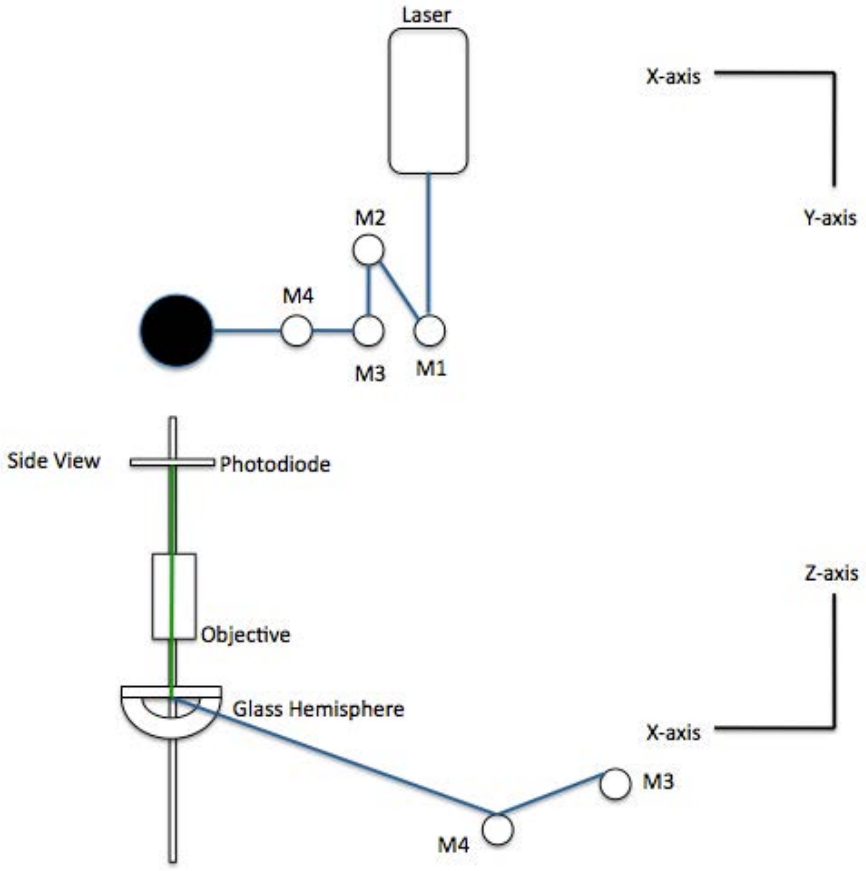

4. Fluorescent Solution and Penetration Depth of Laser in Solution

This project used a fluorescent solution made of Calcein and water. The molar concentration of the Calcein is 0.1 g/L = 0.16mM. The Excitation Coefficient (EC) is approximately 80000 $M^{-1}Km^{-1}$ at 488 nm (the wavelength for the laser used in this project). $T = 10^{EC*l}$, and EC=12.8 cm^{-1}. Thus, after traveling 1mm, the intensity of the laser in this solution is down by a factor of about 10.

Appendix 2

1. Matlab function for the auto correlation of model images at a zero time lag

```
function AverageZeroTimeLag(movie)

global c
global average
global r
global sol

x=zeros(207,207);

for i=1:59
image1=movie(:,:,1,i);
size(image1);
a=(ones(104,1))*(mean(image1));
image1a=image1-a;

image2=movie(:,:,1,i);
b=(ones(104,1))*(mean(image2));
image2a=image2-b;

c(:,:,i)=xcorr2(image1a, image2a);
end

  for i=1:207
    for j=1:207
      for k=1:59
    x(i,j)=x(i,j)+c(i,j,k);
    average=x./i;
      end
    end
  end
plot(average)

figure
for x=1:length(average)
   for y=1:length(average)
     r(x,y)=sqrt(((x-104)^2)+((y-104)^2));
   end
end

g=@(h) sum(sum((average-(h(1).*exp(-(r.^2)./(2.*(h(2)^2))))).^2));
```

```
sol=fminsearch(g,[1.59*10^5, 5]);

s=(sol(1).*exp(-(r.^2)./(2.*(sol(2)^2))));

plot(s)
```

2. **Matlab function for the auto correlation of model images at a 5 second time lag**

```
function AverageFiveSecTimeLag(movie)

global f
global image1a
global image2a
global averagef
global x
global r
global sol

x=zeros(207,207);

for i=1:54
   image1=movie(:,:,1,i);
   size(image1);
   a=(ones(104,1))*(mean(image1));
   image1a=image1-a;

      for j=i+5
         image2=movie(:,:,1,j);
         b=(ones(104,1))*(mean(image2));
         image2a=image2-b;
      end

      f(:,:,i)=xcorr2(image1a, image2a);
end

   for i=1:207
      for j=1:207
         for k=1:54
     x(i,j)=x(i,j)+f(i,j,k);
     averagef=x./i;
         end
      end
   end
   plot(averagef)
```

```
  figure

for x=1:length(averagef)
   for y=1:length(averagef)
     r(x,y)=sqrt(((x-104)^2)+((y-104)^2));
   end
end

g=@(h) sum(sum((averagef-(h(1).*exp(-(r.^2)./(2.*(h(2)^2))))).^2));


sol=fminsearch(g,[1.59*10^5, 5]);

s=(sol(1).*exp(-(r.^2)./(2.*(sol(2)^2))));

plot(s)
```

3. Matlab function for the auto correlation of model images at a 10 frame lag

```
function AverageTenSecTimeLag(movie)

global z
global image1a
global image2a
global averagez
global x
global r
global sol

x=zeros(207,207);

for i=1:49
  image1=movie(:,:,1,i);
  size(image1);
  a=(ones(104,1))*(mean(image1));
  image1a=image1-a;

    for j=i+10
      image2=movie(:,:,1,j);
      b=(ones(104,1))*(mean(image2));
      image2a=image2-b;
    end

    z(:,:,i)=xcorr2(image1a, image2a);
end
```

```
for i=1:207
   for j=1:207
      for k=1:49
  x(i,j)=x(i,j)+z(i,j,k);
  averagez=x./i;
      end
   end
end
plot(averagez)


figure

for x=1:length(averagez)
   for y=1:length(averagez)
     r(x,y)=sqrt(((x-104)^2)+((y-104)^2));
   end
end

g=@(h) sum(sum((averagez-(h(1).*exp(-(r.^2)./(2.*(h(2)^2))))).^2));


sol=fminsearch(g,[1.59*10^5, 5]);

s=(sol(1).*exp(-(r.^2)./(2.*(sol(2)^2))));

plot(s)
```

4. Description of Labview/Matlab program that takes a photon history record

A. Labview program

The front panel displays a plot for the number of photons counted over a time of 200 seconds for channels A and B, (which are connected to PFI0 and PFI3 NI USB-621x, make sure to keep track of which channel is connected where), and the amplitude of the laser voltage. It also displays a numerical value for the maximum voltage recorded from the laser (which is connected to AI15). The user must manually input the number of samples desired for the data acquisition.
Now looking at the block diagram, the number of samples is inputted to DAQ Assistant 1, 2, and 3 which are the DAQ Assistants corresponding to AI15, PFI0, and PFI3 respectively. All of the DAQ Assistants turn the data from an analog signal to a numerical value. DAQ Assistant 1 returns a maximum and a minimum value of the input array, which I will call VoltageArray and creates an index for each value. VoltageArray is then multiplied by 16383, and rotates the elements of VoltageArray

1 place, i.e. VoltageArray(0) becomes VoltageArray(1) and the last element in the array becomes VoltageArray(0). Next, the program deletes VoltageArray(0). In the finals steps, the program converts VoltageArray to a 16-bit integer, and writes the data to a binary file. DAQ Assistant 2 and 3 return maximum and minimum values for their input arrays as well. Since both parts of this code do the same thing, I will just use the name ChannelArray. The elements of ChannelArray are also rotated 1 place, and then ChannelArray(0) is deleted. Instead of a 16-bit integer, ChannelArray is converted to an 8-bit integer and is written to the same binary file as VoltageArray. PFI0 is written to the binary file first, then PFI3, and then AI15.

B. Matlab function used to turn the Labview binary data into decimal data

```
function [A, B, Laser]=labviewBin2Dec(data)

Bbin=data(1:199992); %Bbin is the PFI0 binary data
Bbin=reshape(Bbin, [8, 24999]);
p=2.^(7:-1:0);
B=p*Bbin; %B is decimal data

Abin=data(200000:399991); %Abin is the PFI3 binary data
Abin=reshape(Abin, [8, 24999]);
A=p*Abin; %A is decimal data

LaserBin=data(399999:799982); %LaserBin is the AI15 binary data
LaserBin=reshape(LaserBin, [16,24999]);
p2=2.^(15:-1:0);
Laser=p2*LaserBin; %Laser is the decimal laser power data
```

(See the following pages for the Front Panel and the Block Diagram).

Front Panel

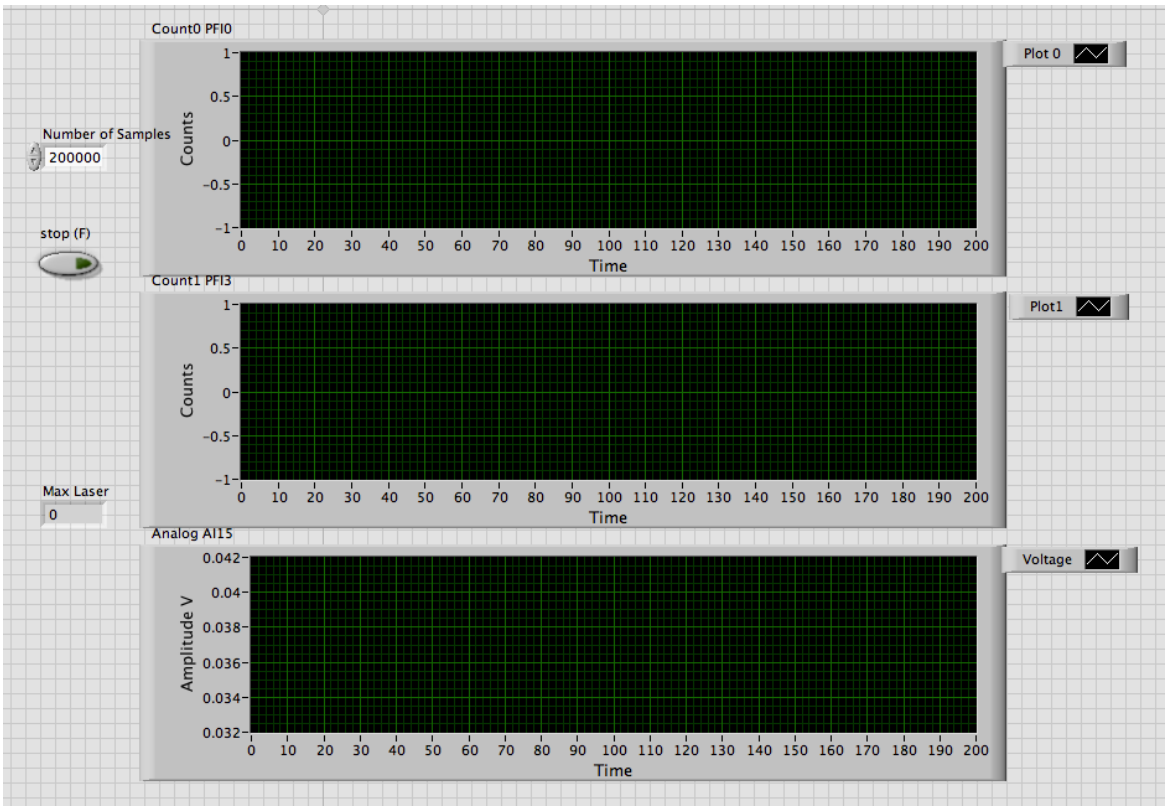
Count0 PFI0
Plot 0
Counts
Time
Number of Samples
200000
stop (F)
Count1 PFI3
Plot1
Counts
Time
Max Laser
0
Analog AI15
Voltage
Amplitude V
Time

Block Diagram

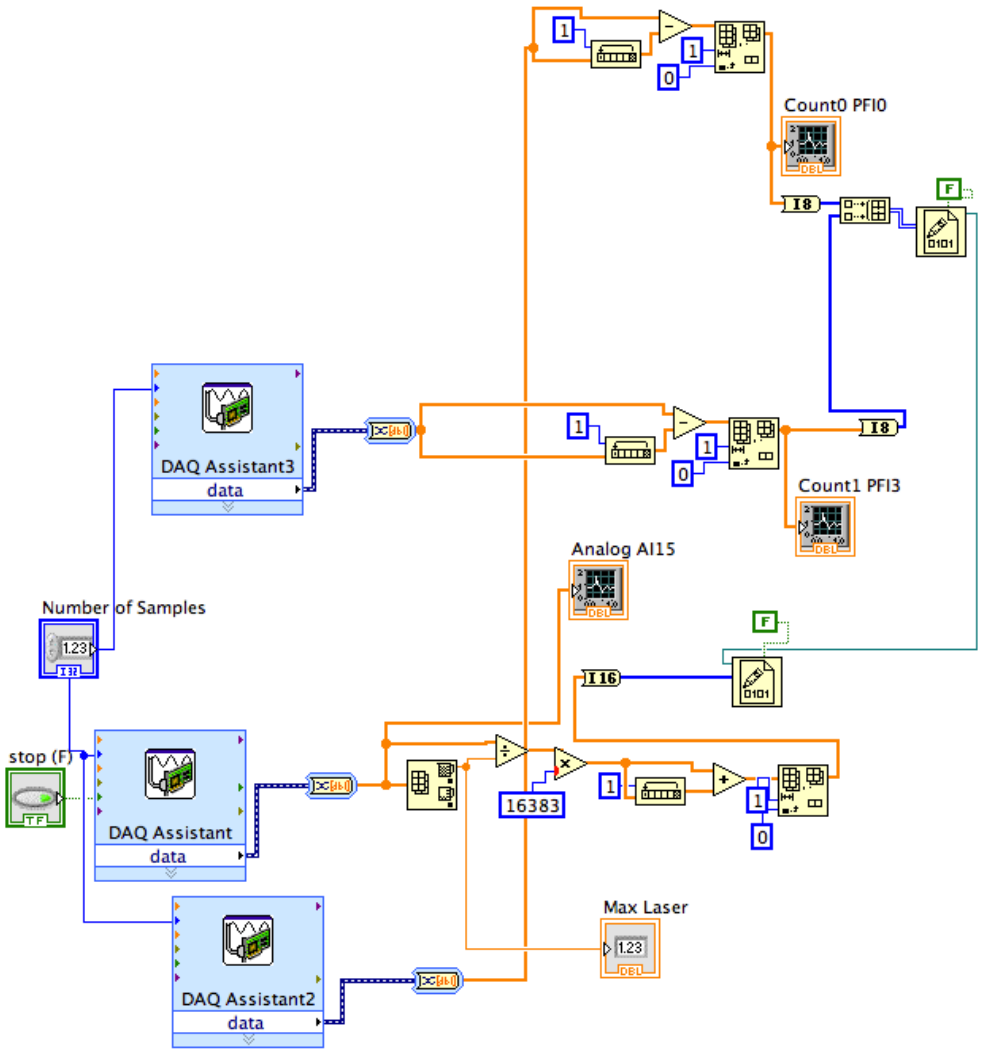

Appendix 3

1. Links for information about products used in this project

1. Nikon Inverted Microscope Eclipse TE200
   http://www.techinst.com/pub_docs/manuals/Biological/TE200%20IM.PDF

2. 63X Zeiss Plan-Apochromat Objective
   https://www.micro-shop.zeiss.com/?a=v&f=o&id=440762-9904-000&l=en&m=s&p=us

3. 20X Mitutoyo Plan Apo NIR Infinity-Corrected Objective
   http://www.edmundoptics.com/microscopy/infinity-corrected-objectives/mitutoyo-nir-nuv-uv-infinity-corrected-objectives/46404/

4. A User Guide for Avalanche photodiodes
   http://www.excelitas.com/downloads/app_apd_a_user_guide.pdf

5. NI USB-621x User Manual
   http://www.ni.com/pdf/manuals/371931f.pdf